

What has brain diffusion MRI taught us about chronic pain: a narrative review

Paul Bautin^{1,3, #}, Marc-Antoine Fortier^{1,3, #}, Monica Sean^{1,3}, Graham Little⁶, Marylie Martel³, Maxime Descoteaux⁶, Guillaume Léonard^{4,5}, Pascal Tétreault*^{1,2,3}

1. Department of Anesthesiology, Faculty of medicine and health sciences, Université de Sherbrooke, Sherbrooke, Quebec, Canada

2. Department of Nuclear medicine and radiobiology, Faculty of medicine and health sciences, Université de Sherbrooke, Sherbrooke, Quebec, Canada

3. Centre de recherche du Centre hospitalier universitaire de Sherbrooke, Sherbrooke, Quebec, Canada

4. School of rehabilitation, Faculty of medicine and health sciences, Université de Sherbrooke, Sherbrooke, Quebec, Canada

5. Research Centre on Aging du Centre intégré universitaire de santé et de services sociaux de l'Estrie – Centre hospitalier universitaire de Sherbrooke, Sherbrooke, Quebec, Canada

6. Sherbrooke Connectivity Imaging Lab (SCIL), Computer Science Department, Université de Sherbrooke, Sherbrooke, Quebec, Canada

* Corresponding author

co-first authors

Corresponding author:

Pascal Tétreault

Université de Sherbrooke, Faculté de médecine et des sciences de la santé

3001, 12e Avenue Nord, Sherbrooke (Québec) J1H 5N4

Tel. (819) 346-1110 x15183

Email: pascal.tetreault@usherbrooke.ca

Number of text pages: 32

Number of figures and tables: 9

Keywords: brain, chronic pain, Magnetic Resonance Imaging (MRI), diffusion MRI, white matter

Running title: Diffusion MRI of the Brain in Chronic Pain

46 **Abstract**

47

48 Chronic pain is a pervasive and debilitating condition with increasing implications for
49 public health, affecting millions of individuals worldwide. Despite its high prevalence, the
50 underlying neural mechanisms and pathophysiology remain only partly understood. Since
51 its introduction 35 years ago, brain diffusion MRI has emerged as a powerful tool to
52 investigate changes in white matter microstructure and connectivity associated with
53 chronic pain. This review synthesizes findings from 58 articles that constitute the current
54 research landscape, covering methodologies and key discoveries.

55

56 We discuss the evidence supporting the role of altered white matter microstructure and
57 connectivity in chronic pain conditions, highlighting the importance of studying multiple
58 chronic pain syndromes to identify common neurobiological pathways. We also explore
59 the prospective clinical utility of diffusion MRI, such as its role in identifying diagnostic,
60 prognostic, and therapeutic biomarkers.

61

62 Further, we address shortcomings and challenges associated with brain diffusion MRI in
63 chronic pain studies, emphasizing the need for the harmonization of data acquisition and
64 analysis methods. We conclude by highlighting emerging approaches and prospective
65 avenues in the field that may provide new insights into the pathophysiology of chronic pain
66 and potential new therapeutic targets.

67

68 Due to the limited current body of research and unidentified targeted therapeutic strategies,
69 we are forced to conclude that further research is required. However, we believe that brain
70 diffusion MRI presents a promising opportunity for enhancing our understanding of
71 chronic pain and improving clinical outcomes.

72

73 **Introduction**

74

75 Over the past 25 years, significant progress has been made in the understanding of chronic
76 pain (CP), particularly with respect to the integral role of brain processes ¹. While many
77 studies have now thoroughly documented the effects of various CP conditions on both brain
78 structure and function ^{2,3}, much of this research has concentrated on gray matter alterations.
79 Studies investigating structural changes to white matter (WM) in relation to chronic pain
80 (CP) remain scarce and inconclusive ⁴⁻⁸. This is significant as white matter comprises
81 nearly half of the brain ⁹, has importance in development ¹⁰⁻¹², in function ¹³⁻¹⁵, in learning
82 ¹⁶ and is known to be impaired in numerous neurological conditions — including
83 Alzheimer's, Parkinson's, depression, multiple sclerosis, and traumatic brain injury ¹⁷⁻²².

84

85 In line with trends in other scientific disciplines, the search for accurate biomarkers is a
86 major focus within the pain research community. The increasing quality and availability of
87 neuroimaging data makes it one of the most promising avenues for the development of
88 biomarkers ^{3,23-27}. Notably, longitudinal and machine learning approaches have yielded
89 significant insights into brain characteristics that predict placebo response ²⁸, longitudinal
90 pain symptom change ²⁹ and transition from subacute phase to CP ³⁰.

91

92 Although the primary focus here is on the white matter, findings from other modalities can
93 contextualize the study of WM in CP. Utilizing structural Magnetic Resonance Imaging
94 (MRI) techniques, such as T1- and T2-weighted imaging, researchers have identified
95 common and distinct brain features across various pain conditions ³¹. Even though recent
96 meta-analysis report subtle, spatially distributed alterations in gray matter regions,
97 including the amygdala, thalamus, hippocampus, insula, anterior cingulate cortex, and
98 inferior frontal gyrus across CP conditions ^{32,33}, unique "brain signatures" specific to
99 individual pain conditions have also been observed. For example, patterns of gray matter
100 density co-variation enabled the classification of individual brains to their condition –
101 either chronic back pain (CBP), complex regional pain syndrome (CRPS) or knee
102 osteoarthritis (OA) ³². Interestingly, these structural characteristics extend beyond the
103 traditionally expected somatosensory regions, they are non-randomly distributed and may
104 play a role to both the onset and maintenance of CP -- as seen in individuals transitioning
105 from subacute to chronic low back pain (CLBP) who present smaller amygdala and

106 hippocampi volumes³⁴. Collectively, these observations reinforce the utility of a nuanced
107 and more global, condition-specific approach to chronic pain.

108

109 Studies examining functional MRI (fMRI), such as BOLD-weighted images, also indicate
110 that certain dynamic features of brain activity, at rest or during task, are characteristic of
111 various CP conditions. For instance, fibromyalgia patients show hypersensitivity to visual
112 and pressure stimuli³⁵⁻³⁷, whereas chronic lower back pain (CLBP) patients display distinct
113 patterns of nucleus accumbens (NAc) activity in response to noxious stimuli³⁸. At the level
114 of resting-state networks, fMRI studies have primarily emphasized changes in the default
115 mode network, driven largely by sustained pain signaling via the medial prefrontal cortex
116³⁹. Emerging research on dynamic connectivity further underscores the significance of
117 looking at brain dynamics, revealing that dynamic features are more predictive of pain
118 experiences than their static counterparts⁴⁰. Given these observations, examining the way
119 white matter (WM) architecture constrains gray matter and functional alterations could
120 offer valuable insights for the development and individualization of novel therapeutic
121 interventions. Interestingly, some of these brain features appear to be plastic, displaying
122 the capacity to partially reverse and reorganize either upon receiving treatment or as the
123 condition progresses^{34,41,42}.

124

125 Diffusion magnetic resonance imaging (dMRI), which measures the signal loss due to the
126 diffusion of water molecules in biological tissues as diffusion-sensitizing gradients are
127 applied⁴³, stands as the most promising non-invasive tool for investigating structural
128 changes in white matter. Introduced in the late 1980s, advancements in dMRI
129 methodologies have been substantial⁴⁴, leading to increasingly sophisticated models for
130 measuring white matter microstructure and reconstructing white matter connectivity. Early
131 implementations primarily relied on calculating the Apparent Diffusion Coefficient
132 (ADC), a scalar measure computed by averaging apparent diffusion on 1 to 3 directional
133 dMRI scans⁴⁵. While these rapid scan sequences have become standard in clinical
134 evaluations of specific pathologies like strokes and tumors, they lack specificity to define
135 the microstructure and are rarely used for the evaluation of chronic pain patients. By the
136 late 1990s, Diffusion Tensor Imaging (DTI)⁴⁶ was introduced, building on the limitations
137 of ADC. By acquiring dMRI images in at least 6 directions, DTI can reconstruct diffusion

138 directional preference, enabling the computation of metrics such as Fractional Anisotropy
139 (FA) and Mean Diffusivity (MD). Nevertheless, in the context of tractography, DTI has
140 limitations in capturing complex fiber configurations such as crossing or kissing fibers. To
141 address this, High Angular Resolution Diffusion Imaging (HARDI) was developed in the
142 early 2000s⁴⁷. By acquiring dMRI in at least 45 directions, HARDI was designed to resolve
143 complex intravoxel structures.

144

145 Despite these advancements, the field of chronic pain (CP) has yet to yield the full potential
146 of diffusion MRI-based methods. Diffusion tensor imaging (DTI) remains the most
147 prevalent method in the field, so much so that it is frequently used as a synonym for dMRI
148 in literature. However, for the community to update its methods, a cautionary note is
149 warranted: if HARDI and multi-shell protocols gain widespread acceptance without
150 standardization, there is a risk of exacerbating variability and noise in the CP literature.
151 Therefore, the aim of this review is to critically assess the existing research concerning the
152 characteristics of brain white matter revealed through diffusion MRI techniques. We
153 examine impairments in white matter across various chronic pain conditions, as defined by
154 the International Association for the Study of Pain (IASP), drawing upon findings from the
155 58 articles that met our inclusion criteria^{48,49}.

156

157 **Methods**

158

159 **Information source**

160 PubMed and Scopus databases were interrogated for articles dated up to 10th March 2022.

161 Articles were also searched using the Medical Subject Headings (MeSH) term on PubMed.

162

163 **Review strategy**

164 This review follows the recommendations from the Preferred Reporting Items for

165 Systematic reviews and Meta-Analyses extension for Scoping Reviews (PRISMA-ScR)

166 Checklist. Search strategies were developed with a librarian of the Health Sciences Library

167 of the Université de Sherbrooke. The keywords chosen for the review were: “magnetic

168 resonance imaging”, “diffusion”, “pain”, and “brain”. The full search strategy can be

169 viewed in the *supplementary material* (supp 1.).

170

171 **Study strategy and inclusion/exclusion criteria**

172 The process for selecting studies in this investigation is depicted in Figure 1. First, from a

173 collection of 447 papers, we discarded reviews and any articles that did not explicitly

174 mention "diffusion," "brain," or "pain" in their title or abstract. Second, we eliminated case

175 studies, non-English articles, and those in which pain was not the main focus. Third, we

176 removed studies if they did not employ diffusion MRI (dMRI) to examine brain regions in

177 individuals suffering from chronic pain or if the study population included participants

178 under the age of one, veterans, amputees, recipients of deep brain stimulation (DBS),

179 individuals with traumatic brain injury (TBI), postoperative patients, stroke or

180 neurodegenerative disease-induced chronic pain sufferers, or subjects experiencing

181 experimentally induced acute pain. Methodological articles and animal studies were also

182 excluded. Fourth, we separated the remaining articles into three categories: chronic primary

183 pain, chronic secondary pain based on the IASP classification^{48,49}, or articles missing

184 information about the chronic pain condition, and only included articles on chronic primary

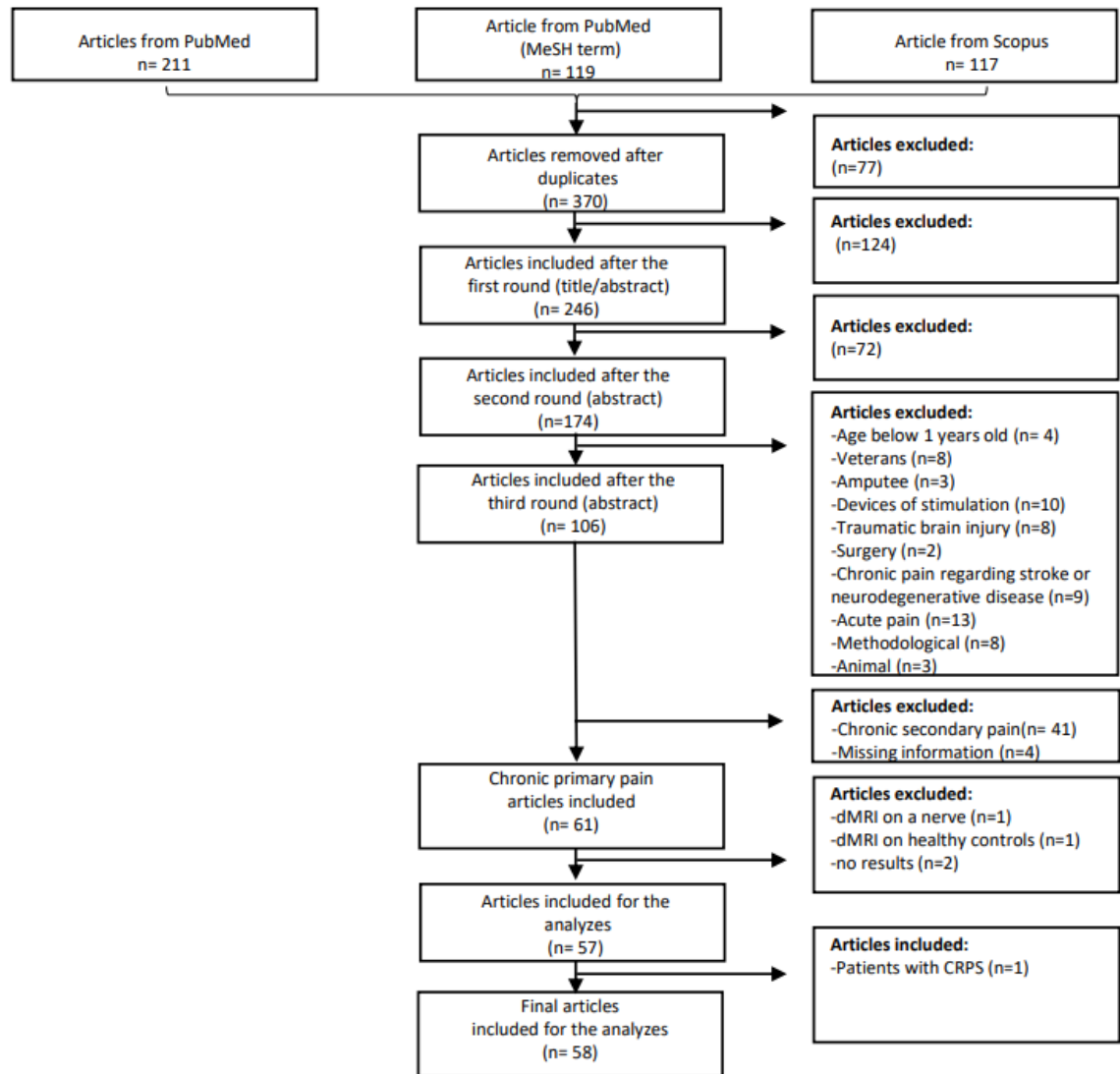
185 pain. We further excluded studies that limited dMRI analysis solely to peripheral nerves,

186 those that included only healthy control subjects, or those that failed to report results (a

187 note on acute pain was also added in *supplementary material [supp 2.]*). Finally, an

188 additional article was incorporated post hoc; this article had been referenced multiple times

189 in the selected literature and was identified as pertinent due to its focus on the use of dMRI
190 in chronic pain, despite not being retrieved by our initial search terms in its title or abstract.



191

192 *Figure 1. Flowchart of the article selection process, 58 final articles were included for*
193 *the analyzes in this review.*

194

195 **Study selection and analyses**

196 The first three steps described in the section “*study strategy and inclusion and exclusion*
197 *criteria*” were conducted by MS and PT; any disagreement was resolved between MS and
198 PT. Subsequently, the classification into primary chronic pain and secondary chronic pain
199 was made by MS and supported by PT and GL. The remaining articles were then separated
200 into five categories based on the IASP classification: (i) chronic widespread pain; (ii)

201 complex regional pain syndrome; (iii) chronic primary headache or orofacial pain; (iv)
 202 chronic primary visceral pain and (v) chronic primary musculoskeletal pain. If applicable,
 203 half of the articles in each category were separated and respectively analyzed by MS and
 204 PT. The remaining articles were analyzed by MM and GLe. Finally, each reviewer (MS,
 205 PT, MM and GLe) extracted, based on the chart developed by PT, general study design
 206 information and dMRI-specific study data.
 207

	Term	Definition
Local reconstruction methods	ADC -- Apparent Diffusion Coefficient	A measure used in MRI that reflects the magnitude of diffusion (of water molecules) within tissue in mm ² /s.
	DTI -- Diffusion Tensor Imaging	A technique that models the local diffusion of water in each voxel as a Gaussian distribution or ellipsoid. The three primary eigenvectors and eigenvalues of the tensor characterize the main diffusion directions and magnitudes. Common metrics derived from DTI include fractional anisotropy, colored fractional anisotropy, axial diffusivity, mean diffusivity and radial diffusivity (FA, RGB, AD, MD, and RD) ⁴⁶ .
	CSD -- Constrained Spherical Deconvolution	An approach that reconstructs the fiber orientation distribution function (fODF) in each voxel. This is achieved by deconvolving the diffusion signal with a fiber response function ⁵⁰ .
	NODDI -- Neurite orientation and dispersion density imaging	A method that represents the neurite orientation dispersion and density within each voxel. It utilizes a three-compartment tissue model: intracellular, extracellular, and cerebrospinal fluid isotropic compartments ⁵¹ .
Tractography reconstruction	Deterministic tractography	A tractography approach that solely follows the most likely fiber orientation when propagating the streamlines (seeding from the same location will always reconstruct the same streamline).
	Probabilistic tractography	A tractography technique that probabilistically samples the fiber orientation representation during the streamline propagation process.
	Seeding and tracking mask regions	These terms refer to the specific regions where streamline propagation starts (seeding) and the designated areas it is permitted to navigate through (tracking mask).
Analysis method	TBSS -- Tract Based Spatial Statistics	A method designed to generalize voxelwise statistical analysis for DTI metric maps. This is achieved by projecting all subjects' FA data onto a mean FA tract skeleton, followed by applying voxelwise cross-subject statistics ^{52,53} .
	Tractometry	A technique that quantifies diffusion metrics along specific fiber bundles ^{54,55} .
	ROI – Region of Interest Analysis	A method that segments distinct regions of interest within an image or dataset, facilitating focused analysis on specific brain structures or areas.

	VBA – Voxel Based Analysis	A technique employed to discern regional differences by juxtaposing measurements at the voxel level through registration.
Connectivity analysis	NBS – Network Based Statistics	A method developed to control for multiple comparisons when mass-univariate testing is executed on network edge connections ^{56,57} .
	Graph Theory Metrics	A collection of mathematical measurements and algorithms tailored for the analysis and description of networks or graphs. Common metrics are small worldness and degree, among others.

208 *Table 1. Glossary of technical dMRI terms*

209

210 **Results**

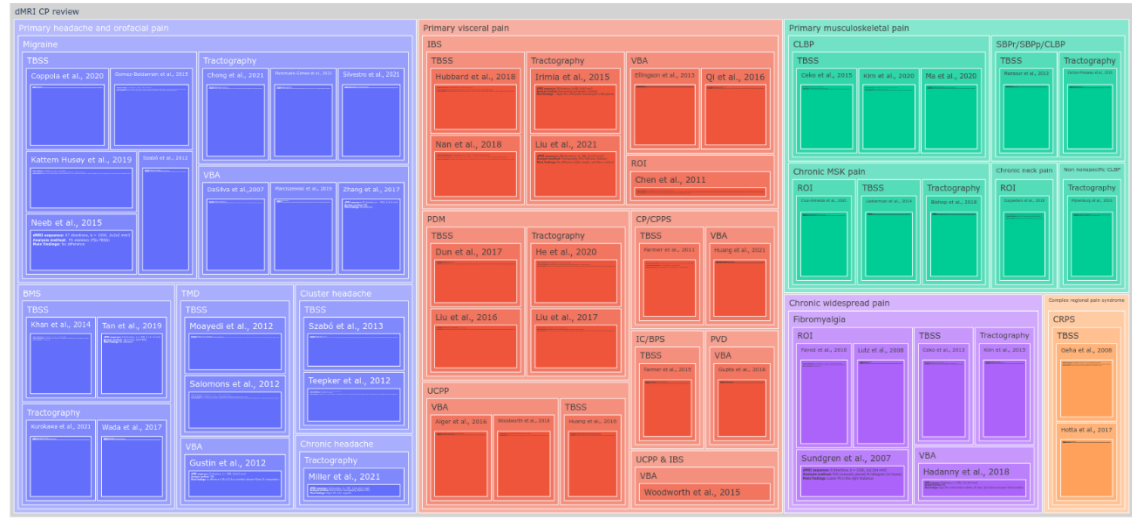
211 Of the 370 unique articles initially identified, 246 articles remained after removing reviews
 212 and articles which did not fit our inclusion criteria for the title and abstract. Subsequent
 213 removal of case-reports, articles not available in English and articles that only reported
 214 pain anecdotally yielded a total of 174 articles. Further exclusion of articles that did not
 215 acquire dMRI in brain regions or on a specified chronic pain condition population, left 106
 216 articles. Then, the remaining articles were separated into three categories: chronic primary
 217 pain (61 articles), chronic secondary pain (41 articles) and articles missing information
 218 about the chronic pain condition (4 articles); only chronic primary pain articles were kept.
 219 Afterwards, we excluded articles where the dMRI was acquired: on a nerve, only on
 220 healthy participants and articles without results, leaving 57 articles. Finally, one previously
 221 omitted article was added retrospectively because it was cited several times by the
 222 remaining articles, giving a total of 58 articles for the final analysis. Figure 2 presents an
 223 interactive overview of 58 articles that met our inclusion criteria regrouped according to
 224 the latest IASP chronic pain definition and their analysis method.

225 In the interest of clarity and conciseness, a list of all abbreviations used in the results is
 226 provided below (Table 2). Furthermore, abbreviations are redefined at the beginning of
 227 every section as not all chronic pain types may pertain to the interest of the reader.

Abbreviation	Definition	Abbreviation	Definition
ACC	Anterior cingulate cortex	IC	Internal capsule
CC	Corpus callosum	JHU	Johns Hopkins University
CR	Corona radiata	PAG	Periaqueductal gray
CST	Corticospinal tract	ROI	Region of interest
EC	External capsule	SLF	Superior longitudinal fasciculus
IFOF	Inferior fronto-occipital fasciculus	S1	Somatosensory cortex

ILF Inferior longitudinal fasciculus

228 **Table 2.** Abbreviations of regions of interest
229



230
231 **Figure 2.** An interactive overview of 58 articles that met our inclusion criteria regrouped
232 according to the latest IASP chronic pain definition and their analysis method. In **blue**:
233 primary headache and orofacial, **red**: primary visceral pain, **green**: primary
234 musculoskeletal pain, **purple**: chronic widespread pain and **orange**: complex regional pain
235 syndrome. Dynamic figure can be found here: <https://osf.io/4wyqt/>

236
237 **Chronic primary headache or orofacial pain**

238 The IASP classification defines chronic primary headache or orofacial pain as headache or
239 orofacial pain manifesting for at least 15 days per month and persisting for over three
240 months. The duration of untreated daily pain is a minimum of two hours or may manifest
241 in multiple shorter episodes⁴⁸. In reviewing this category, 21 articles were identified: 11
242 focused on migraine^{58–68}, two on cluster headache^{69,70}, one on chronic headache⁷¹, three
243 on temporomandibular disorder (TMD)^{72–74} and four on burning mouth syndrome^{75–78}.

244
245 In the studies examining **migraine**, five investigations employed FSL-TBSS for voxel-
246 wise statistical analyses on whole-brain fractional anisotropy (FA) skeletons^{58,64–67}. While
247 Neeb et al.⁶⁴ and Coppola et al.⁶⁵ solely relied on TBSS, Kattrem Husøy et al.⁵⁸ and Szabó
248 et al.⁶⁷ incorporated additional tractography analyses. Gomez-Beldarrain et al.⁶⁶ further
249 extended their approach to include a region-of-interest (ROI) analysis, utilizing both white

250 and gray matter atlases. Neeb et al. reported no significant differences in FA, mean
251 diffusivity (MD), axial diffusivity (AD), and radial diffusivity (RD) between migraine
252 patients and healthy controls. Coppola et al. examined both episodic and chronic migraines,
253 finding no FA differences in episodic migraine patients but identifying higher RD and MD
254 in bilateral superior and posterior corona radiata (CR), the bilateral genu of the corpus
255 callosum (CC), the bilateral posterior limb of the internal capsule (IC) bilateral superior
256 longitudinal fasciculus (SLF) in chronic migraine patients. Kattem Husøy et al. discovered
257 elevated AD in major tracts, most notably in the bilateral CC, corticospinal tract (CST),
258 inferior fronto-occipital fasciculus (IFOF), inferior longitudinal fasciculus (ILF), and left
259 SLF. They also noted lower volumes in the CC and IFOF when employing deterministic
260 tractography, but only in the new-onset headache group. Szabó et al. found lower FA and
261 higher MD and RD values in frontal white matter bundles. Probabilistic tractography,
262 originating from TBSS seed regions, revealed these bundles to be connected to the
263 orbitofrontal cortex, insula, thalamus, and dorsal midbrain. Gomez-Beldarrain et al.
264 observed lower FA in the TBSS skeleton and identified significantly different TBSS
265 clusters between controls and migraine patients, which were mapped to ROIs in the Johns
266 Hopkins University (JHU) diffusion tensor imaging (DTI)-based Atlas and the MNI
267 structural Atlas. The interior insula, bilateral cingulate gyri, and right uncinate fasciculus
268 were pinpointed as regions with lower FA values.

269 Three investigations exclusively utilized tractography ^{60,63,68}. Chong et al. ⁶⁰ employed
270 probabilistic tractography to segment and average white matter microstructural properties
271 with the aim of differentiating migraine patients from those with post-traumatic headaches.
272 Their predictive model achieved an accuracy rate of 78%; however, no diffusion metrics
273 were compared. Planchuelo-Gomez et al. ⁶³ used probabilistic tractography to build a
274 whole brain connectome by measuring streamline counts between gray matter regions.
275 They observed both higher and lower numbers of streamlines in connections involving
276 specific regions such as the superior frontal gyrus. Additionally, they found variations in
277 FA, AD, and RD in connections involving regions like the hippocampus. Silvestro et al. ⁶⁸
278 took a similar approach, employing probabilistic tractography to construct a whole-brain
279 connectome. They quantified the connection probability between gray matter regions and
280 further examined the resultant connectome using network-based statistics (NBS) and graph
281 theory network analysis. Their findings highlighted nodes with significantly higher

282 connection probabilities in multiple regions, including the precuneus, cuneus, amygdala,
283 calcarine cortex, and posterior cingulate cortex, anterior cingulate cortex (ACC),
284 postcentral gyrus, lingual and fusiform gyri, middle frontal gyrus and inferior and superior
285 parietal lobules.

286 Three investigations utilized voxel-based analysis (VBA) ^{59,61,62}. Zhang et al. ⁵⁹ reported
287 no significant differences using a whole-brain VBA approach via SPM12. On the other
288 hand, Marciszewski et al. ⁶¹ observed elevated MD in various brain regions, including the
289 spinal trigeminal nucleus, dorsal medial/lateral pons, midbrain periaqueductal gray (PAG),
290 and cuneiform nucleus. They also identified higher FA in the white matter regions of the
291 medial lemniscus and ventral trigeminal thalamic tract. Dasilva et al. ⁶² further extended
292 their approach to include a ROI analysis, utilizing both white and gray matter atlases. They
293 discovered lower FA values in specific patient subgroups: the ventro-lateral PAG was
294 affected in migraine patients without aura, while the ventral trigemino-thalamic tract
295 showed reduced FA in migraine patients with aura.

296

297 In the studies examining **cluster headache**, two investigations employed FSL-TBSS for
298 voxel-wise statistical analyses on whole-brain FA skeletons ^{69,70}. Szabo et al. ⁶⁹ reported a
299 significant increase in MD, AD, and RD across widespread white matter regions in the
300 frontal, parietal, temporal, and occipital lobes. They also found reduced FA in the CC and
301 in specific frontal and parietal white matter tracts, such as the bilateral forceps minor and
302 major, the bilateral CR, the IC and external capsule (EC), the cerebral peduncle, the parietal
303 juxtacortical white matter and the IFOF, predominantly on the contralateral side of the
304 pain. Notably, AD exhibited a negative correlation with the frequency of headache attacks.
305 Teepker et al. ⁷⁰ reported alterations in FA in multiple brain regions, including the
306 brainstem, thalamus, IC, superior and inferior temporal regions, frontal lobe, occipital lobe,
307 and cerebellum.

308

309 In one study examining **chronic headache**, conducted by Miller et al. ⁷¹, they used
310 deterministic tractography to segment and average diffusion metrics on tracts. They
311 observed higher FA in the cingulum.

312

313 In the studies examining **temporomandibular disorders (TMD)**, two investigations
314 employed FSL-TBSS for voxel-wise statistical analyses on whole-brain FA skeletons^{72,73}.
315 Both studies extended their analysis to include tractography. Moayed et al.⁷³ went further
316 by also incorporating VBA. Salomons et al.⁷² conducted their analysis using TBSS and
317 then segmented major tracts via probabilistic tractography. They observed that FA values
318 in connected white matter tracts along the CST were associated with feelings of
319 helplessness; however, no group comparison of diffusion metrics were reported. Moayed
320 et al., after performing TBSS analyses, employed probabilistic tractography, using seed
321 regions identified from significant TBSS clusters, to measure connection probability. They
322 also applied a whole-brain VBA. Their findings indicated lower FA in the anterior limb of
323 the IC and the EC. Additionally, they observed a higher connection probability from the
324 CC to the frontal pole and a lower connection probability from the CC to the dorsolateral
325 prefrontal cortex.

326 One investigation exclusively utilized whole-brain VBA⁷⁴. Gustin et al.⁷⁴ observed no
327 significant differences in FA within the primary somatosensory cortex (S1), nor did they
328 find any correlation between FA and reorganization of S1.

329

330 In the studies examining **burning mouth syndrome (BMS)**, two investigations employed
331 FSL-TBSS for voxel-wise statistical analyses on whole-brain FA skeletons^{76,77}. Khan et
332 al.⁷⁶ extended their study by incorporating probabilistic tractography to segment major
333 white matter tracts. They found no significant differences in either TBSS-based diffusion
334 metrics or average tract metrics and volumes. Tan et al.⁷⁷, who solely employed TBSS,
335 also found no significant differences in the whole-brain FA skeleton.

336 Two investigations exclusively utilized tractography to construct whole brain connectomes
337^{75,78}. Both used probabilistic tractography to measure the streamline count between gray
338 matter regions and subsequently applied graph theory network analysis methods to further
339 examine the connectomes. Wada et al.⁷⁵ observed localized changes in connectivity within
340 the ACC and prefrontal cortex, specifically in the medial orbitofrontal cortex and pars
341 orbitalis. They also noted strengthened connections between the ACC and medial
342 prefrontal cortex with regions such as the basal ganglia, thalamus, and brainstem. Despite
343 these findings, no significant differences were observed in graph theory metrics. Kurokawa
344 et al.⁷⁸ reported increased connectivity and betweenness centrality in the left insula, right

345 amygdala, and right lateral orbitofrontal cortex as well as reduced betweenness centrality
346 and connectivity in the right inferotemporal cortex.

347

348

349 **Chronic primary visceral pain**

350 The IASP classification defines chronic primary visceral pain as persistent or recurrent
351 pain (for longer than three months) that occurs in the internal organs of the head (or neck)
352 region and of the thoracic, abdominal, or pelvic cavities, unexplained by any other
353 condition ⁴⁸. The pain anatomical location corresponds with typical referral pain patterns
354 from specific internal organs. It can manifest in diverse forms, such as pain in the digestive
355 system, the thoracic region, and the abdominal region, as well as pelvic pain originating
356 from the viscera of the digestive, urinary, and genital systems. In this category, 19 studies
357 were included. Among them, four focused on primary dysmenorrhea (PDM) ⁷⁹⁻⁸², seven
358 on irritable bowel syndrome (IBS) ⁸³⁻⁸⁹, four on urologic chronic pelvic pain (UCPP) ⁹⁰⁻⁹³,
359 two on prostatitis/chronic pelvic pain syndrome (CCP/CPPS) ^{94,95}, one on cystitis/bladder
360 pain syndrome ⁹⁶ and one on provoked vestibulodynia (PVD) ⁹⁷.

361

362 In the studies examining **primary dysmenorrhea (PDM)**, two investigations employed
363 FSL-TBSS for voxel-wise statistical analyses on whole-brain fractional anisotropy (FA)
364 skeletons ^{79,82}. While both studies utilized TBSS, Liu et al. ⁸² extended their analysis to
365 include tractography. Dun et al. ⁷⁹ observed lower FA values, alongside higher mean
366 diffusivity (MD) and radial diffusivity (RD), across various white matter fibers tracts.
367 These tracts included the splenium part of the corpus callosum (CC), the posterior limb of
368 the internal capsule (IC), the superior and posterior of the corona radiata (CR), as well as
369 the posterior thalamic radiation. Conversely, Liu et al. reported higher FA and lower MD
370 and RD values, primarily in the CC, fornix, bilateral IC, bilateral external capsule (EC),
371 CR, and bilateral posterior thalamic radiation, bilateral sagittal stratum, right cingulum and
372 bilateral superior longitudinal fasciculus (SLF). In addition, tractography was employed by
373 Liu et al. to visually inspect connectivity originating from TBSS seed regions.

374 Two investigations exclusively utilized tractography ^{80,81}. Both studies performed
375 tractography in a population atlas to manually segment white matter tracts of interest.
376 Subsequently, these segmentations were registered to the native space for a region-of-

377 interest (ROI) analysis of diffusion tensor imaging (DTI) metrics. He et al.⁸⁰ reported
378 lower FA values in connections between the thalamus and somatosensory cortex (S1) as
379 well as between the thalamus and insula. Conversely, they found higher FA values in the
380 tracts connecting the thalamus to the dorsal anterior cingulate cortex (ACC) and the
381 supplementary motor area. Liu et al.⁸¹ observed lower FA and axial diffusivity (AD), along
382 with higher RD and MD, in a specific cluster located in the dorsal posterior cingulum and
383 in the parahippocampal segment of the cingulum bundle.

384

385 In the studies examining **irritable bowel syndrome (IBS)**, three investigations employed
386 FSL-TBSS for voxel-wise statistical analyses on whole-brain FA skeletons⁸⁶⁻⁸⁸. Chen et
387 al.⁸⁷ further refined their TBSS analysis with a ROI approach using multiple atlases,
388 including the Johns Hopkins University (JHU) white matter atlas, Harvard-Oxford cortical
389 structural atlas, MNI structural atlas, Talairach Daemon labels, and the Juelich histological
390 atlas. Similarly, both Hubbard et al.⁸⁶ and Nan et al.⁸⁸ employed an ROI-based approach,
391 albeit solely using the JHU white matter atlas for segmentation. Chen et al. observed higher
392 FA values in the fornix and EC adjacent to the right posterior insula. Hubbard et al., while
393 not finding any significant differences in the whole FA skeleton, did report lower FA in
394 the lower dorsal cingulum; however, they found no variations in MD and RD values. Nan
395 et al. reported lower FA and higher RD specifically in the genu of the CC, with no observed
396 differences in MD.

397 Two studies exclusively employed tractography methods^{83,89}. Irimia et al.⁸³ utilized
398 deterministic tractography to calculate average tract DTI metrics while Liu et al.⁸⁹ applied
399 tractography originating from the bilateral posterior cingulate gyrus to compute metrics
400 such as average tract FA, fiber length, and streamline count. Irimia et al. observed higher
401 FA values in white matter bundles innervating the S1. In contrast, Liu et al. did not report
402 any significant differences in their measured parameters.

403 Two studies employed voxel-based analysis (VBA)^{84,85}. Ellingson et al.⁸⁴ extended their
404 analysis by incorporating a ROI approach using the JHU atlas and applied probabilistic
405 tractography to compute the number of streamlines between certain atlas ROIs. Qi et al.⁸⁵
406 similarly extended their analysis by applying tractography but originated it from fMRI-
407 defined ROI clusters to compute average tract DTI metrics, streamline count, and path
408 length. Ellingson et al. observed higher FA values in various grey matter regions including

409 the globus pallidus, putamen, medial thalamus, and sensory and motor cortices as well as
410 in white matter regions such as the primary cortical projections from the thalamus,
411 posterior cingulate, frontal lobe and ACC white matter and CC when using VBA. They
412 also reported higher MD within the globus pallidus, IC, thalamus, CR, and areas connected
413 to sensory, pre-frontal, and posterior parietal regions. In terms of tract density, they found
414 higher values in tracts connecting the thalamus to the prefrontal cortical regions and the
415 medial dorsal nuclei to the ACC. Conversely, they observed lower tract density in
416 connections between the globus pallidus and the thalamus. In contrast, Qi et al. did not find
417 any significant differences in path length, tract count, or FA within the fibers connecting
418 the bilateral ventral ACC to the inferior parietal lobules.

419

420 In the studies examining **urologic chronic pelvic pain (UCPP)**, one study conducted by
421 Huang et al. ⁹¹ utilized FSL-TBSS for voxel-wise statistical analyses on whole-brain FA
422 skeletons. Huang et al. extended their TBSS analysis by incorporating a ROI approach
423 using the JHU white matter atlas. Huang et al. reported lower FA and higher AD values in
424 the thalamic radiation but found no significant differences in either MD or RD.

425 Three studies employed VBA ^{90,92,93}. The 2018 study by Woodworth ⁹² focused solely on
426 whole-brain VBA, while the 2015 Woodworth study ⁹⁰ extended its analysis to include
427 probabilistic tractography. Alger et al. ⁹³ incorporated a ROI approach using the JHU white
428 matter atlas. In the 2018 study, Woodworth reported significant correlations between DTI
429 measures and urinary protein quantifications; however, no comparative analyses were
430 conducted between different groups in terms of diffusion metrics. The 2015 Woodworth
431 study found lower FA, lower generalized FA, lower tract density, and higher MD in brain
432 regions typically associated with the perception and integration of pain information.
433 Interestingly, the study did not compare IBS patients to a control group but did find them
434 to be significantly different from UCPP patients. Alger et al. primarily aimed to evaluate
435 the variability in FA measurements. Their study obtained data from various acquisition
436 sites for neurologic chronic pain syndrome in healthy controls but did not conduct any
437 comparative analyses on diffusion metrics.

438

439 In the studies examining **prostatitis/chronic pelvic pain syndrome (CCP/CPPS)**, one
440 study utilized FSL-TBSS for voxel-wise statistical analyses on whole-brain FA skeletons

441 ⁹⁴. Farmer et al. ⁹⁴ reported no significant differences in whole-brain FA skeletons across
442 various DTI measures.

443 In a single study conducted by Huang et al. ⁹⁵, both VBA and tractography were employed
444 to calculate whole-brain connectome and graph theory metrics. Huang et al. observed lower
445 global efficiency in the right middle frontal gyrus (orbital part) and higher global efficiency
446 in the left middle cingulate and paracingulate gyrus. Additionally, they reported increased
447 local efficiency in the left middle cingulate and paracingulate gyri, as well as the
448 paracentral lobule.

449

450 In the study examining **cystitis/bladder pain syndrome**, a study utilized FSL-TBSS for
451 voxel-wise statistical analyses on whole-brain FA skeletons ⁹⁶. Farmer et al. ⁹⁶ reported
452 lower FA values in specific regions: the right thalamic radiation, the left forceps major,
453 and the right longitudinal fasciculus. Conversely, they observed higher FA in the right SLF
454 as well as in the bilateral inferior longitudinal fasciculus (ILF).

455

456 In the study examining **provoked vestibulodynia (PVD)**, a study conducted by Gupta et
457 al. employed VBA on the whole brain and a ROI approach with the Harvard-Oxford
458 subcortical atlas to segment gray matter regions ⁹⁷. The investigators reported extensive
459 increases in FA within the somatosensory and basal ganglia regions as well as variations
460 in MD specifically in the basal ganglia.

461

462 **Chronic primary musculoskeletal pain**

463 The IASP classification defines chronic primary musculoskeletal pain as persistent or
464 recurrent (for longer than three months) pain that occurs in the muscles, bones, joints, or
465 tendons ⁴⁸. A classic example is chronic primary low-back pain. This category is further
466 subclassified based on pain anatomical location, including the upper back as chronic
467 primary cervical pain, the mid-back as chronic primary thoracic pain, the lower back as
468 chronic primary low-back pain, and the limbs as chronic primary limb pain. In this
469 category, ten studies were included. Among them, five focused on sub-acute/chronic low
470 back pain (SBP/CLBP) ^{34,98–101}, three on chronic musculoskeletal pain syndrome ^{102–104},
471 one on nonspecific low back pain ¹⁰⁵ and one on chronic neck pain ¹⁰⁶.

472

473 In the studies examining **sub-acute/chronic low back pain (SBP/CLBP)**, four studies
474 employed FSL-TBSS to conduct voxel-wise statistical analyses on whole-brain fractional
475 anisotropy (FA) skeletons^{98–101}. Among these, Kim et al.¹⁰¹ solely employed TBSS,
476 Mansour et al.⁹⁸ extended their analysis to include tractography, and both Ma et al.⁹⁹ and
477 Ceko et al.¹⁰⁰ applied a region of interest (ROI) approach. Specifically, Ma et al. utilized
478 a white matter atlas for their ROI analysis, while Ceko et al. employed ROI clusters derived
479 from a prior fMRI study. Kim et al. observed that CLBP patients exhibited reduced FA in
480 both the somatosensory cortex (S1)-back and S1-finger regions when compared to controls
481 by averaging FA skeleton diffusion tensor imaging (DTI) metrics in ROIs. Mansour et al.
482 found lower FA values in three distinct clusters: one in the temporal part of the superior
483 longitudinal fasciculus (SLF), a second in the left retro-lenticular part of the internal
484 capsule (IC), and a third involving the left anterior limb of the IC as well as portions of the
485 corpus callosum (CC), including the anterior corona radiata (CR) in SBP patients with pain
486 that persisted compared to SBP patients that recovered after a year. Ma et al. reported lower
487 FA in several regions: the CC, bilateral anterior and right posterior thalamic radiation, right
488 SLF, and left anterior CR among CLBP patients. Contrarily, Ceko et al. didn't find any
489 whole-brain DTI metric differences in the FA skeleton, but instead measured an increased
490 FA in the left insula post-treatment.

491 One study exclusively used probabilistic tractography to reconstruct the whole brain
492 connectome and evaluate the number of connections and connection probabilities³⁴.
493 Vachon-Preseau et al.³⁴ observed higher density of connections between corticolimbic
494 regions, such as the nucleus accumbens, the amygdala, the hippocampus and the prefrontal
495 cortex in patients with pain that persisted compared to SBP patients that recovered after a
496 year. No comparisons were made with respect to DTI metrics.

497

498 In the studies examining **non-specific chronic low back pain (NSCLBP)**, Pijnenburg et
499 al.¹⁰⁵ study exclusively used probabilistic tractography to reconstruct the whole brain
500 connectome and evaluate graph theory network analysis. The investigators observed lower
501 local efficiency in NSCLBP cases; notably, no comparative analysis was conducted on
502 diffusion metrics.

503

504 In the studies examining **chronic musculoskeletal pain**, two studies employed FSL-TBSS
505 to conduct voxel-wise statistical analyses on whole-brain FA skeletons^{102,103}. Lieberman
506 et al.¹⁰³ extended their analysis by incorporating a ROI approach using a white matter atlas.
507 Bishop et al.¹⁰² also employed an ROI approach using the JHU white matter atlas, a whole
508 brain fixel-based analysis and a probabilistic tractography with constrained spherical
509 deconvolution (CSD) reconstruction of the whole-brain connectome to apply network-
510 based statistics (NBS). Lieberman et al. found no significant differences in FA or axial
511 diffusivity (AD) in the whole-brain TBSS FA skeleton. However, they reported higher
512 radial diffusivity (RD) in multiple regions, including the body of the CC, right SLF and
513 both anterior and posterior limbs of the IC. Further ROI analyses revealed lower FA in the
514 splenium of the CC and the left temporal lobe branch of the cingulum bundle adjacent to
515 the hippocampus. Elevated RD was also found in several regions, such as the splenium of
516 the CC, the right limbs of the IC, part of the external capsule (EC) adjacent to the insular
517 cortex, the SLF and the cerebral peduncle. Bishop et al. observed lower F1 values in the
518 right EC, right SLF, and right uncinate fasciculus, as well as lower F2 values in the left
519 cingulum and the splenium of the CC (F1 and F2 are respectively the first and second fiber
520 population partial volume fractions, these diffusion properties can only be calculated when
521 using advanced diffusion models that can account for multiple crossing fibers within a
522 voxel). They also found lower mode of anisotropy in several areas including the splenium
523 of the CC, left cerebral peduncle, and bilateral EC. In their whole-brain TBSS skeleton
524 analysis, no differences in F1 and F2 were found. However, fixel-based analysis revealed
525 reduced fiber density in the splenium of the CC and the right temporal lobe white matter
526 region of the inferior frontal-occipital fasciculus (IFOF). No differences were observed in
527 fiber cross-section. Utilizing a connectome approach, Bishop et al. reported increased
528 connectivity between several regions, including the hippocampus, parietal cortex,
529 thalamus, precuneus, and visual cortex structures like the calcarine and cuneus gray matter.
530 One study exclusively used an ROI approach, utilizing DTI and neurite orientation
531 dispersion and density imaging (NODDI) metrics¹⁰⁴. By targeting ROIs within both white
532 matter and gray matter atlases, Cruz-Almeida et al.¹⁰⁴ observed lower orientation
533 dispersion index values in the white matter of several regions, including the anterior CR,
534 right posterior thalamic radiation, uncinate fasciculus, superior cerebellar penduncle, and
535 fornix.

536

537 In a study focused on **chronic neck pain**, conducted by Coppieters et al. ¹⁰⁶, an ROI
538 approach using a white matter atlas was employed to assess DTI metrics. The investigation
539 revealed no significant differences in ROI-based DTI metrics between patients with
540 chronic neck pain and healthy controls.

541

542

543 **Chronic widespread pain**

544 The IASP classification defines chronic widespread pain as persistent or recurrent (for
545 longer than three months) diffuse musculoskeletal pain that occurs in a minimum of four
546 body regions and in at least three of four body quadrants (upper–lower/left–right side of
547 the body) ^{48,107}. In this category, six studies were included. All of which focused on
548 fibromyalgia (FM) ^{108–113}.

549

550 In the studies focused on fibromyalgia, one study conducted by Ceko et al. ¹⁰⁹ utilized FSL-
551 TBSS for voxel-wise statistical analyses on whole-brain fractional anisotropy (FA)
552 skeletons. Additionally, they employed tractography to examine connectivity originating
553 from significant TBSS clusters. While no differences were observed in whole-brain FA
554 skeletons with respect to diffusion tensor imaging (DTI) measures, the investigators did
555 report lower FA in regions adjacent to areas where significant gray matter volume
556 differences were identified.

557 One study exclusively used tractography to construct whole brain connectomes using
558 streamline counts between gray matter regions ¹¹⁰. Kim et al. ¹¹⁰ used probabilistic
559 tractography to build a whole brain connectome by measuring streamline count between
560 gray matter regions. Notably, they found no differences in the white matter fiber count
561 connecting areas associated with hyperalgesia and clinical pain (no local diffusion metrics
562 were compared).

563 One study exclusively used a whole brain voxel-based analysis (VBA) ¹¹¹. Hadanny et al.
564 ¹¹¹ observed higher FA in several regions, including the anterior thalamic radiation, left
565 insula, right thalamus, and superior thalamic radiation.

566 Three studies exclusively used region of interest (ROI) based analysis methods ^{108,112,113}.
567 Sundgren et al. ¹⁰⁸ used ROI masks for the whole brain and manually placed ROI spheres

568 to utilize a histogram comparison method. Their findings included lower FA in the right
569 thalamus, with no significant results for apparent diffusion coefficient (ADC). Fayed et al.
570 ¹¹² also manually positioned ROI spheres to compare FA and ADC metrics but found no
571 significant differences between groups. Lutz et al. ¹¹³ manually segmented ROIs to
572 compare FA and ADC metrics. They observed lower FA in both the thalami,
573 thalamocortical tracts, and both insular regions, alongside higher FA in the postcentral gyri,
574 amygdala, hippocampi, superior frontal gyri, and anterior cingulate gyri. No significant
575 differences were found in ADC metrics.

576

577

578 **Complex regional pain syndrome (CRPS)**

579 The IASP classification defines complex regional pain syndrome (CRPS) as persistent, or
580 recurrent (for longer than three months) pain characterized by its regional distribution and
581 time course. The pain typically begins distally in an extremity following trauma and is
582 disproportionate in both magnitude and duration when compared to the usual course of
583 pain after similar tissue injuries ^{48,114,115}. While two subtypes of CRPS have been identified,
584 they are beyond the scope of this review. In this category, two studies were included ^{116,117}.

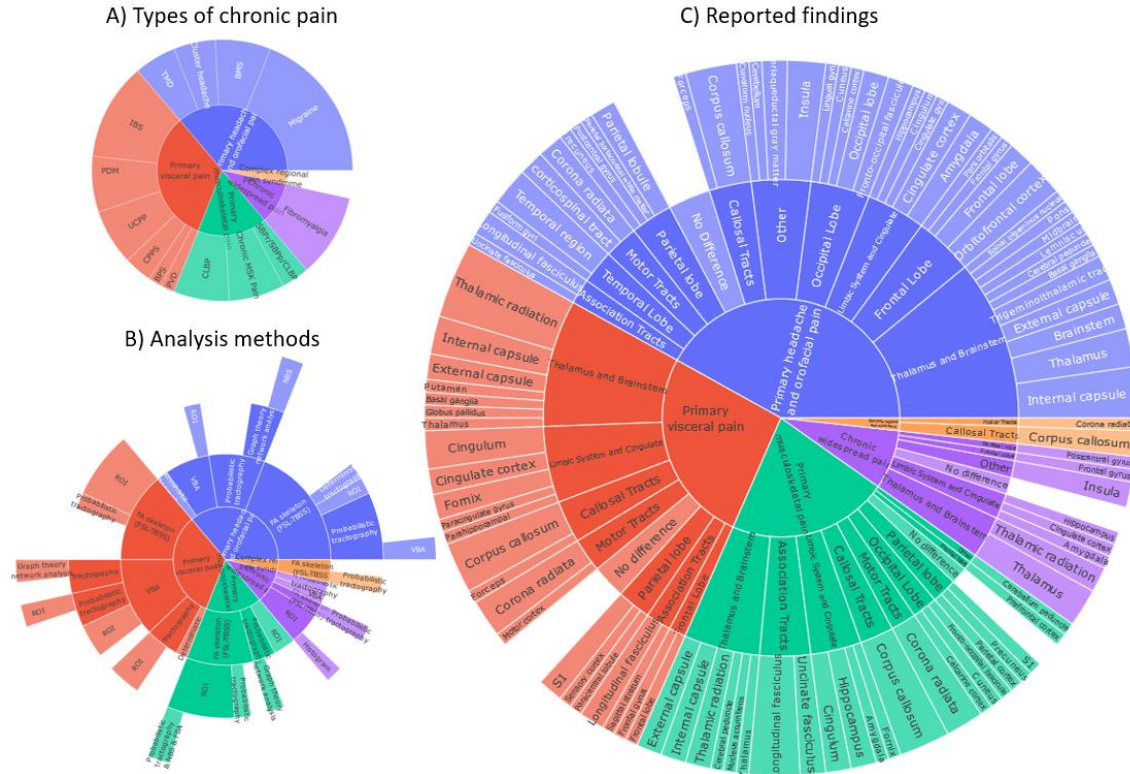
585

586 In the studies focused on **Complex regional pain syndrome (CRPS)**, two studies
587 employed FSL-TBSS for voxel-wise statistical analyses on whole-brain fractional
588 anisotropy (FA) skeletons ^{116,117}. While both studies used TBSS, Geha et al. ¹¹⁷ extended
589 their approach to include probabilistic tractography, which was applied to investigate
590 connectivity originating from voxel-based morphometry (VBM) seed regions. Geha et al.
591 reported a lower FA cluster within the left callosal fiber tract. Hotta et al. ¹¹⁶, who solely
592 utilized TBSS, observed higher mean diffusivity (MD), axial diffusivity (AD), and radial
593 diffusivity (RD) in the genu, body, and splenium of the corpus callosum (CC) as well as in
594 the left anterior, posterior and right superior parts of the corona radiata (CR). Across the
595 whole-brain FA skeletons, they observed average lower FA, higher MD and RD, and no
596 differences were observed in AD.

597

598 **Summary of our findings**

599 To illustrate the results covered in this review, we have provided a summary of the types
 600 of chronic pain, the analysis methods and the reported regions and tracts used for the study
 601 of chronic pain with diffusion MRI in figure 3.
 602

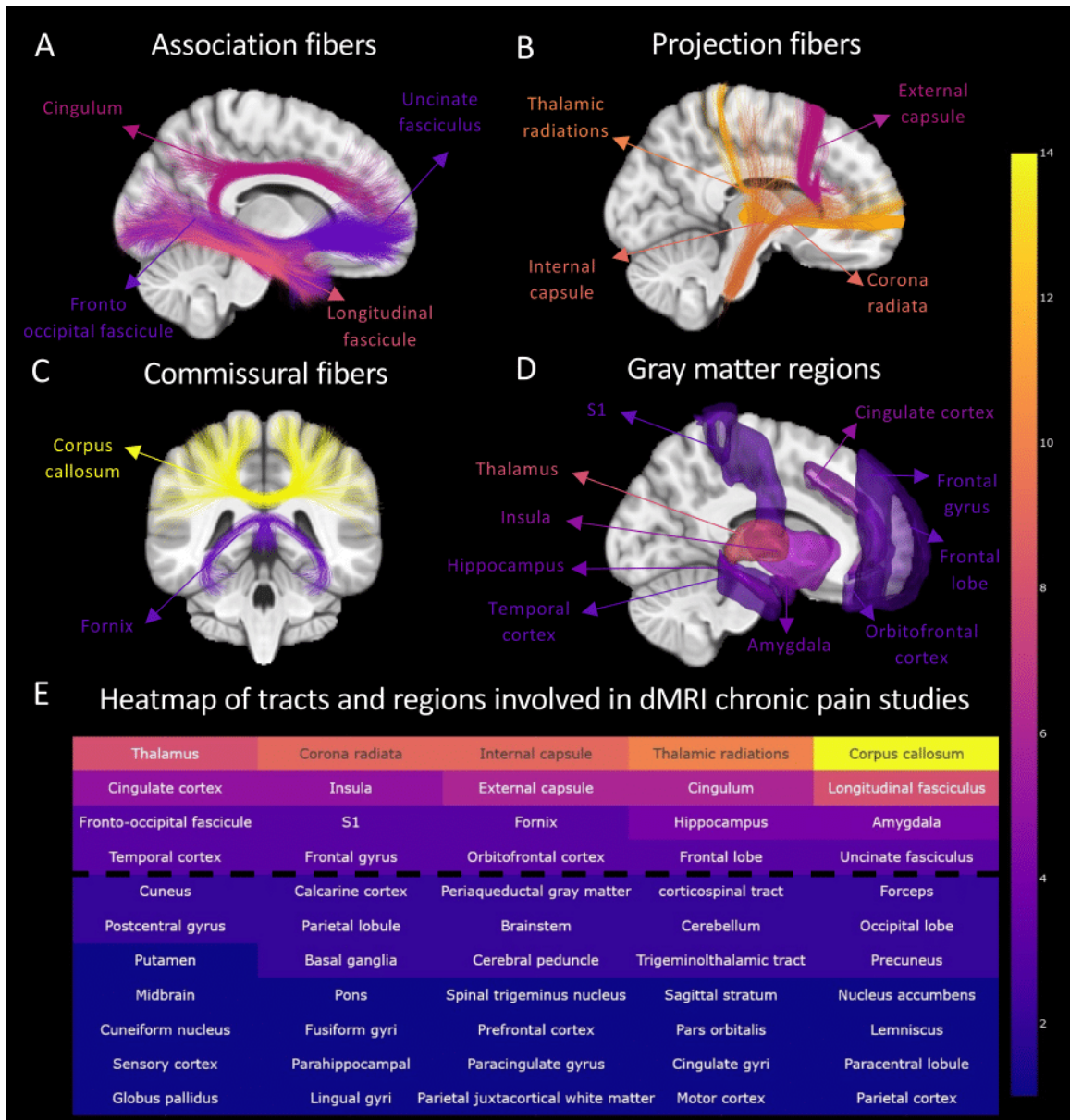


603 **Figure 3.** An interactive visual summary of the reviewed studies in terms of the types of
 604 chronic pain studied (A), the used analysis methods (B) and the tracts and regions
 605 reported as significant findings (C). In **blue**: primary headache and orofacial, **red**:
 606 primary visceral pain, **green**: primary musculoskeletal pain, **purple**: chronic widespread
 607 pain and **orange**: complex regional pain syndrome. Dynamic figure can be found here:
 608 <https://osf.io/4wyqt/>
 609
 610

611
 612 **Discussion**

613
 614 The purpose of this review was to provide a critical summary of the use of brain dMRI for
 615 the study of primary chronic pain conditions. Each article was classified according to the
 616 latest IASP chronic pain definition, dMRI sequence and analysis method. The main
 617 findings of this review highlight the difficulty of delineating common white matter
 618 abnormalities for each chronic pain condition. Indeed, as shown by figure 4, sixty-four
 619 percent (35/55) of all reported regions/tracts are only reported once or twice across all

620 studies. Furthermore, the variety of reported metrics for a given region accentuates the lack
621 of consensus of white matter properties for each chronic pain condition. This observation
622 comes in part from the vast number of possibilities to analyze and further report results
623 from dMRI data. Notwithstanding, some regions are reported more consistently. For
624 example, the corpus callosum is reported in twenty-four percent (14/58) of all studies and
625 a few tracts and regions emanating from the thalamus are reported in over 10% of all
626 studies. However, these findings must be interpreted with caution as these regions could
627 either be relatively easier to investigate (due to size, shape and localization), more common
628 in the pain literature and subject to “publication bias”¹¹⁸ as the average study CP subjects
629 sample size is relatively low (37 subject/study)¹¹⁸.

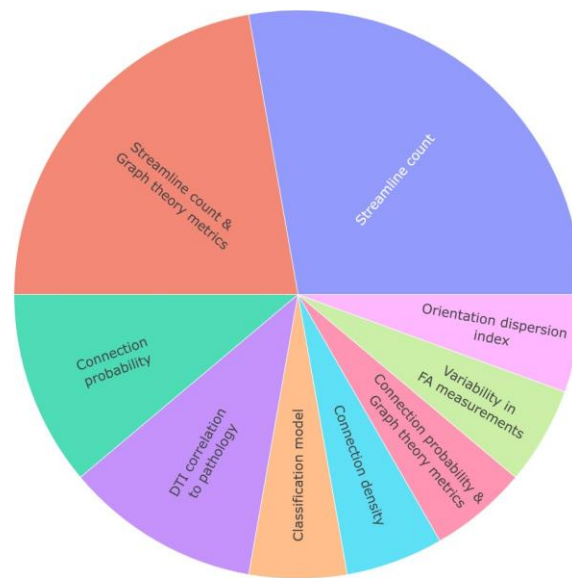


630

631 *Figure 4. Visual representation of the association fibers (A), the projection fibers (B), the*
 632 *commissural fibers (C) and the gray matter regions (D) which were mentioned by at least*
 633 *three different articles in this review (above the dashed line in the heatmap). (E) An*
 634 *interactive heatmap of how consistently each tract and region is reported as significant*
 635 *findings across the studies of this review. The tracts and regions with warm colors (towards*
 636 *yellow) are reported more consistently (with a maximum of 14 studies that report the*
 637 *corpus callosum) relatively to tracts and regions with cold colors (towards blue; with over*
 638 *50% of regions mentioned only once or twice). Dynamic heatmap can be found here:*
 639 <https://osf.io/4wyqt/>

640

641 Seventy-nine percent of studies (46/58) have used DTI metrics group comparisons between
642 CP and healthy controls as part of their reported findings. While this seems to be a common
643 first step, thirty-one percent of studies (18/58) reported further analyses than DTI metric
644 group comparisons (seven articles in the orofacial pain category, seven articles in the
645 visceral pain category, three articles in the musculoskeletal pain category and one article
646 in the widespread pain category). These additional analysis methods are highlighted in
647 figure 5 to illustrate the diversity of dMRI analysis approaches.



648

649 *Figure 5. Distribution of alternative metrics to diffusion metrics comparisons between*
650 *chronic pain (CP) and healthy controls used in diffusion MRI. Dynamic figure can be found*
651 *here: <https://osf.io/4wyqt/>*

652

653 Interestingly, twenty-four percent of the studies (14/58) reported no differences between
654 the groups that were investigated. Of these, five were in the orofacial pain category (two
655 migraine, one TMD and two BMS studies), two in the musculoskeletal pain category (one
656 CLBP and one chronic neck pain), five in the visceral pain category (three IBS, one UCPP
657 and one CP/CPPS) and two on widespread pain (fibromyalgia).

658

659 Finally, six percent of the studies (4/59) reported differences of FA or ODI in the fornix
660 (two in visceral pain, one in CRPS and one in MSK) even though, due to its unique location
661 surrounded by CSF, it is most likely affected by partial volume effects (PVE) even when

662 using state-of-the art dMRI acquisition sequences ¹¹⁹. Furthermore, as presented later,
663 when using a TBSS approach, the fornix is almost absent from the TBSS FA skeleton.

664

665 **Main critics of the approaches used in the 58 articles**

666

667 **Acquisition parameters**

668 Diffusion MRI metrics, though quantitative, are somewhat restricted in terms of their
669 sensitivity and specificity. This necessitates careful interpretation of these metrics,
670 considering methodological, technical, and biological factors. A notable issue affecting
671 the consistency and reliability of dMRI is the substantial variation in scanning parameters
672 across different studies. For instance, a recent study explored the variability in diffusion-
673 weighted MRI across multiple sites, scanners, and subjects. The study demonstrated that,
674 under specific acquisition conditions, the variability between different scanners assessing
675 the same subject could be comparable to the variability between different subjects assessed
676 on the same scanner ¹²⁰. As for any MRI sequences, many parameters need to be properly
677 chosen to ensure high-quality diffusion-sensitive images. Three key parameters
678 significantly influence both dMRI image quality and the outcomes of their subsequent
679 analyses: 1) the b-value; representing the strength, duration and timing of the diffusion
680 encoding gradients ^{43,121}; 2) the number of diffusions encoding gradient directions;
681 generally representing the number of diffusion gradient directions applied over a sphere
682 ^{122,123}; and 3) the voxel dimensions; representing the length, width and height of the 3D
683 image voxels ¹²⁴. For reference, the most common acquisition parameters used for DTI are
684 in the range of a b-value of 1000 s/mm², 30 unique gradient directions and a 2mm isotropic
685 resolution.

686

687 1) Across studies, the b-value parameter was the most stable with ~75% of studies using a
688 b-value of 1000 s/mm². However, some studies reported b-values in an unusual range—
689 such as 700, 800, 900, 1200, and 1300 s/mm²—without providing any explanation.
690 Additionally, certain studies failed to report the b-value at all. Strikingly, only two groups
691 performed multi-shell acquisitions, an acquisition strategy introduced over 15 years ago
692 ¹²⁵, which allows for state-of-the-art dMRI analysis. Using modern multiband sequences,

693 multi-shell images for whole brain in-vivo imaging can be acquired in an acceptable
694 amount of time -- between 10 and 20 minutes at most.

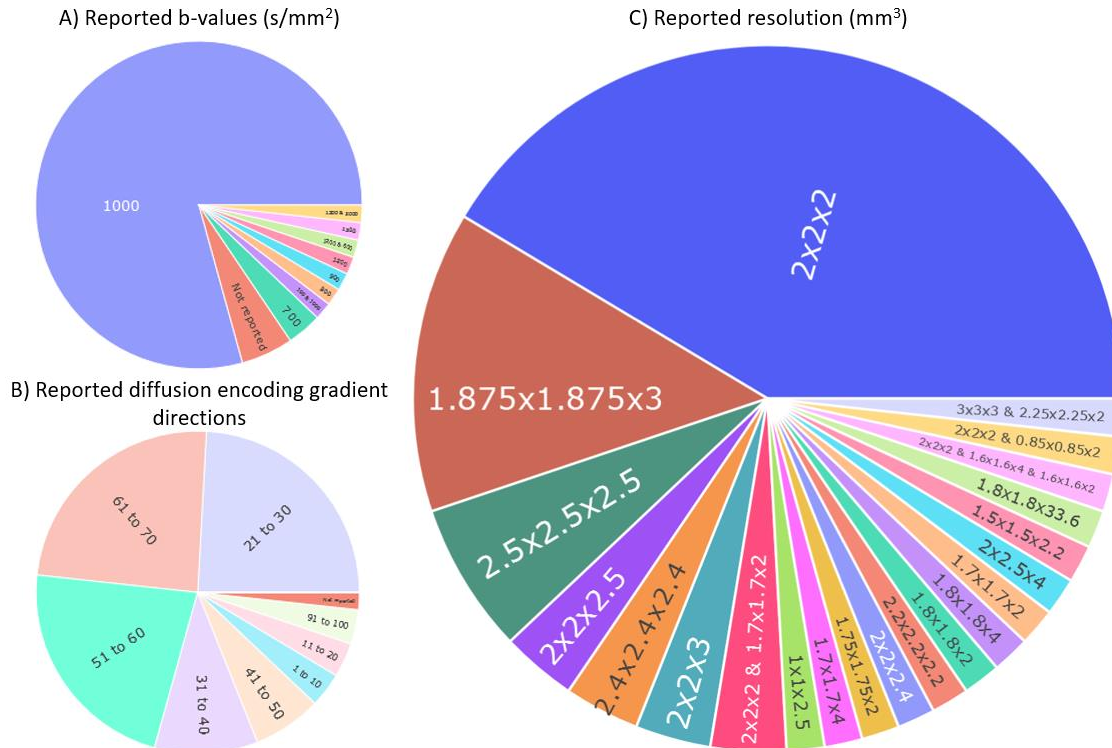
695

696 2) When investigating the number of diffusion encoding gradient directions, we found that
697 approximately 55% of the studies acquired a minimum of 30 directions (with a maximum
698 of 99 directions). This parameter, however, exhibited significant variability; some studies
699 used as few as six or nine directions. This is of concern because the theoretical minimum
700 required to adequately describe a diffusion tensor is six gradient directions ^{126,127}. In the
701 broader context of tractography and fiber orientation estimation, high angular resolution
702 diffusion imaging (HARDI) has emerged as an effective acquisition strategy designed to
703 address the limitations of traditional diffusion tensor imaging (DTI) ^{128,129}. Based on the
704 acquisition of over 50 gradient directions at a single high b-value, HARDI (even when
705 paired with a multi-shell acquisition) can be completed in a reasonable timeframe, between
706 10 and 20 minutes at most.

707

708 3) Lastly, when investigating image resolution, the overall voxel volume ranged from
709 2.4mm^3 to 20mm^3 . While forty-seven percent of studies used the conventional 2mm
710 isotropic resolution, there was notable variability, with some studies acquiring highly
711 anisotropic voxels -- such as $1.875 \times 1.873 \times 3$ or $2 \times 2.5 \times 4\text{mm}^3$. These anisotropic voxel
712 dimensions can introduce biases into diffusion magnetic resonance imaging (dMRI)
713 analyses. For instance, larger voxels are more likely to contain multiple fiber populations,
714 thereby reducing fiber orientation homogeneity and affecting diffusion metrics ¹²⁴.
715 Additionally, anisotropic voxels can influence tractography algorithms, particularly in
716 situations involving branching fibers¹³⁰.

717



718
719
720
721
722
723

Figure 6. Overview of the different acquisition parameters used in the studies of the review. Distribution of the b-value in s/mm^2 (A), the number of diffusion encoding gradient directions (B) and the resolution in mm^3 (C). Dynamic figure can be found here: <https://osf.io/4wyqt/>

724 Overall, the observations made in this section highlight the heterogeneity of acquisition
725 parameters and pre-processing pipelines across chronic pain dMRI studies. This diversity
726 underscores a critical challenge for the field: the need for a more unified approach that
727 would facilitate comparative and cumulative research. For a recent review of dMRI
728 preprocessing, we refer to article ¹³¹ and for a more detailed characterization of the impact
729 of MRI acquisition parameters on diffusion models, we refer to international benchmark
730 competitions reports, notably that discuss the impact of different inversion time (TI) and
731 echo time (TE) ^{132–134}.

732

733 **Processing and analysis tools**

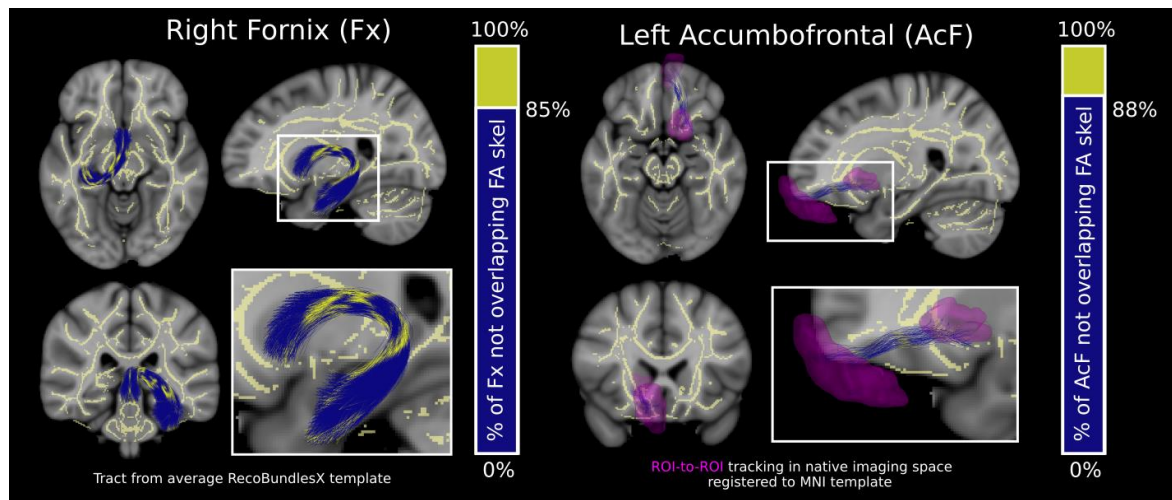
734 The tools provided by the FMRIB group at Oxford were the most used, with over 70% of
735 the papers using one of the FSL tools to process their dMRI data. Almost 50% of the papers
736 use the Tract Based Spatial Statistic (TBSS) pipeline ¹³⁵ to identify voxel-wise differences.
737 Although TBSS is a valid approach that provides significant advantages over classic

738 whole-brain voxel-based analysis when it comes to group comparison, this method does
739 not use the full potential of dMRI images as it summarizes the complexity of the whole-
740 brain white matter into a WM skeleton that is only a few voxels wide. Also, this approach
741 does not completely exclude registration errors ¹³⁶. Therefore, almost no information
742 coming from tracks spanning up to the cortex or tracks that are smaller or located in
743 complex regions can be found in the TBSS maps. The other most commonly used software
744 to process dMRI data were ExploreDTI ¹³⁷ and MRtrix ¹³⁸, both offering advanced tools
745 specifically designed for dMRI data to generate tractography and diffusion metrics maps.
746 To circumvent issues brought by TBSS, some studies presented a clever approach to
747 identify white matter tracts impacted by the chronic pain condition under study. They used
748 the clusters of significant differences identified in the TBSS results as seeds to perform
749 probabilistic tractography. Although this approach allows for the identification of actual
750 white matter tracts that were not present in the WM skeleton, it still cannot reconcile the
751 fact that a significant volume of white matter was not included in the original TBSS
752 analysis. Similarly, several groups identified GM ROIs from fMRI experiments and then
753 expanded this region to include adjacent white matter as a WM ROI to extract diffusion
754 properties. These approaches need to be interpreted carefully as a WM bundle passing close
755 to a GM region does not necessarily connect with that region. Indeed, many WM tracts
756 travel long distances in the brain without connecting with each region they are bordering
757 along the way. A more appropriate approach could have been to use the GM ROI to
758 generate seeds from/to which WM fibers might connect and extract anatomically plausible
759 tracks from a whole brain tractogram.

760

761 To illustrate the constraints of the TBSS methods, we examined the disparities between
762 TBSS and a track-based approach for two specific tracks, namely the fornix and the
763 accumbofrontal (AcF) track, both of which are of particular significance in chronic pain
764 research owing to the regions they connect. Notably, the fornix serves as the primary
765 pathway for efferent signals from the hippocampus, and it plays a critical role in memory
766 circuitry ¹¹⁹. Moreover, hippocampus volume has been shown to be a risk factor in the
767 transition from acute to chronic pain ³⁴. The AcF track connects the orbitofrontal cortex to
768 the nucleus accumbens ¹³⁹, both regions that are also implicated in the transition from acute
769 to chronic pain ³⁰. To demonstrate the benefits of employing targeted approaches for

770 investigating white matter tracks involved in chronic pain, we analyzed the overlap of two
771 streamline bundles extracted using separate techniques with a commonly used whole brain
772 FA skeleton (method described in *supplementary material* [supp 3.]). As a quantitative
773 measure of overlap, voxels intersected by these tracks were extracted and the percentage
774 of voxels overlapping the binarized FA skeleton were output for each track. The fornix and
775 AcF tracks are displayed in Figure 7 along with the percentage of overlapping voxels
776 showing 15% voxels overlap between TBSS and tractography approached for the fornix
777 (figure 7 left), and only 12% voxels overlap for the AcF track (figure 7 right). This analysis
778 was reproduced for a few other subjects from the OpenPain database and similar overlaps
779 were obtained (not shown).
780



782 *Figure 7. A visualization of the overlap between the FSL FA skeleton used commonly in*
783 *whole brain diffusion MRI analysis and two different reconstructed white matter bundles*
784 *taken from two different tractography analysis approaches. The population average right*
785 *fornix (Fx) bundle used in the RecobundleX analysis pipeline is displayed in blue with*
786 *regions overlapping the FA skeleton displayed in yellow. Voxels overlapping the bundle*
787 *were extracted and the percentage of these voxels overlapping the FA skeleton are*
788 *displayed as a bar graph. The same metrics are displayed for the Left Accumbofrontal (AcF)*
789 *track which was generated in native imaging space by extracting tracks that traversed*
790 *ROIs (pink) from the nucleus accumbens and the orbital frontal gyrus. Only a small*
791 *proportion of these tracks overlap the whole brain FA skeleton from FSL, suggesting that*
792 *more targeted analysis approaches may be more sensitive to detecting microstructural*
793 *alterations in some white matter structures.*

794

795

796 **Where should the field go?**

797 Similar to the challenges faced by fMRI for processing and analysis ^{127,130}, dMRI is facing
798 reproducibility and replication issues. As evidenced by the results of this review, there is a
799 substantial degree of variability in published findings, methodologies, and metrics across
800 different studies. While there exists several good guidelines discussing future directions
801 for neuroimaging-based pain biomarker research ^{3,25,140,141}, we suggest specific strategies
802 to address dMRI's challenges: i) updating dMRI signal modelling, ii) increase access and
803 availability of dMRI data for CP, and iii) adopting standardized pipelines specific to dMRI.
804

805 **i) Updating dMRI local reconstruction methods:** To identify and increase group
806 differences, novel biomarkers that increase sensitivity and specificity must be found.
807 Recent advancements in magnetic resonance (MR) hardware and acquisition schemes—
808 such as high angular resolution diffusion imaging (HARDI), diffusion spectrum imaging
809 (DSI), and multi-shell protocols—as well as analysis methods enable the exploration of
810 such brain markers ¹⁴². However, the field of chronic pain (CP) has yet to yield the full
811 potential of these methods. For instance, diffusion tensor imaging (DTI) has been so
812 prevalent that it is often used interchangeably with dMRI in literature. More recent studies
813 in dMRI have moved away from DTI, as it fails to accurately represent multiple fiber
814 populations within a single white matter voxel. The tensor model typically falls short in
815 capturing accurate microstructural information in voxels where fiber crossing occurs; given
816 that this happens in approximately 60 to 90% of all white matter voxels in the brain ¹⁴³, the
817 DTI method is increasingly seen as providing anatomically unsound information –
818 especially when applying tractography. Recent dMRI research has begun to move away
819 from DTI, adopting newer methods aiming for a more precise representation of underlying
820 white matter tissue organization. Within the studies reviewed here, four studies employed
821 whole-brain connectome metrics and two utilized multi-compartment local models. While
822 these newer methods are promising, a caveat is warranted: if HARDI and multi-shell
823 protocols gain widespread acceptance without standardization, there is a risk of
824 exacerbating variability and noise in the CP literature. Notably, the application of these
825 methods on DTI data will most likely provide unreliable results. Therefore, we advocate
826 for the adoption of these advanced techniques only within a structured framework of
827 standardized protocols, reproducible analytical pipelines and cross-validation.

828

829 **ii) Increasing access and availability of dMRI data for pain:** One of the notable
830 challenges in the study of chronic pain using diffusion magnetic resonance imaging (dMRI)
831 is the limited access and availability of extensive open-access datasets. These limitations
832 hamper the statistical power and generalizability of research findings. As such, studies
833 included in this review had a maximum of 103 participants and a minimum of 7 participants
834 (with an average of 37.33 ± 27.39 participants). Recent advancements in the
835 democratization of machine learning methods, in data sharing^{144,145}, in data harmonization
836^{146,147}, and the adoption of uniform metrics present significant opportunities for addressing
837 this issue. By leveraging these advancements, researchers have the potential to rapidly
838 expand and enrich open-access datasets specifically focused on chronic pain.

839

840 **iii) Adopting standardized pipelines specific to dMRI:** Both the field of chronic pain
841 research and diffusion magnetic resonance imaging (dMRI) are subject to large intra-group
842 variability. For chronic pain, such variability can be attenuated by refining the specificity
843 of clinical evaluations, thereby reducing confounds related to the chronic pain condition
844 itself. One approach could be selecting study participants with consistent clinical criteria
845 or ensuring a large enough sample size for data-driven selection. For dMRI, variations can
846 be minimized at every stage, from data collection to analysis. It is important to note that
847 dMRI has specific challenges, unlike other types of structural MR imaging. These
848 challenges include image susceptibility distortions, region-of-interest positioning, image
849 registration, and data smoothing. Conventional structural MR analysis techniques, such as
850 whole-brain voxel-based analysis, might be less suitable due to common dMRI pitfalls¹⁴⁸.
851 Therefore, we recommend that the acquisition parameters, pre-processing, processing and
852 analysis be conducted with standardized pipelines specific to dMRI.

853

854 Overall, the goal of this review was not to favor one method over another but to provide
855 an overview of the current state of the field. However, in writing this review, we emphasize
856 the difficulty of finding commonalities amidst the diverse methods used for image
857 acquisition, analysis, and communication. Consequently, we pinpoint specific areas that
858 require attention and potential improvements. Ultimately, we hope that addressing these
859 challenges will allow pain researchers to capture more reproducible, specific and subtle
860 white matter abnormalities.

861

862 **Limitations**

863 Due to evolving chronic pain definitions and dMRI nomenclature, it is likely that articles
864 performing dMRI on primary chronic pain patients were missed in this review ⁴⁸. Some
865 papers might have identified their participants otherwise had they used these new
866 definitions. For example, an article from Geha et al ¹¹⁷, referenced by other studies in this
867 review, was erroneously excluded because its dMRI nomenclature did not meet our
868 inclusion criteria.

869

870 **Author Approval**

871 All authors have seen and approved the manuscript.

872

873 **Conflicts of interest**

874 MD is co-founder of IMEKA inc.

875 All other authors declare no conflict of interest.

876

877 **Funding**

878 MS is supported by a PhD scholarship from the CIHR. GLi is supported by UNIQUE and
879 NSERC postdoctoral scholarships. PT is supported by FRQS J1 salary award and Arthritis
880 Society star career development award. GLe is supported by FRQS J2 salary award.

881

882 **References:**

883

884

- 885 1. Baliki MN, Apkarian AV. Nociception, pain, negative moods and behavior selection.
886 *Neuron*. 2015;87(3):474-491. doi:10.1016/j.neuron.2015.06.005
- 887 2. Kregel J, Meeus M, Malfliet A, et al. Structural and functional brain abnormalities in
888 chronic low back pain: A systematic review. *Semin Arthritis Rheum*. 2015;45(2):229-
889 237. doi:10.1016/j.semarthrit.2015.05.002
- 890 3. van der Miesen MM, Lindquist MA, Wager TD. Neuroimaging-based biomarkers for
891 pain: state of the field and current directions. *Pain Rep*. 2019;4(4):e751.
892 doi:10.1097/PR9.0000000000000751
- 893 4. Drake-Pérez M, Boto J, Fitsiori A, Lovblad K, Vargas MI. Clinical applications of
894 diffusion weighted imaging in neuroradiology. *Insights Imaging*. 2018;9(4):535-547.
895 doi:10.1007/s13244-018-0624-3
- 896 5. Tae WS, Ham BJ, Pyun SB, Kang SH, Kim BJ. Current Clinical Applications of
897 Diffusion-Tensor Imaging in Neurological Disorders. *Journal of Clinical Neurology*
898 (*Seoul, Korea*). 2018;14(2):129. doi:10.3988/jcn.2018.14.2.129
- 899 6. Nørhøj Jespersen S. White matter biomarkers from diffusion MRI. *Journal of*
900 *Magnetic Resonance*. 2018;291:127-140. doi:10.1016/j.jmr.2018.03.001
- 901 7. Goveas J, O'Dwyer L, Mascalchi M, et al. Diffusion-MRI in neurodegenerative
902 disorders. *Magnetic Resonance Imaging*. 2015;33(7):853-876.
903 doi:10.1016/j.mri.2015.04.006
- 904 8. Kamagata K, Andica C, Kato A, et al. Diffusion Magnetic Resonance Imaging-Based
905 Biomarkers for Neurodegenerative Diseases. *Int J Mol Sci*. 2021;22(10):5216.
906 doi:10.3390/ijms22105216
- 907 9. Fields RD. Change in the Brain's White Matter. *Science*. 2010;330(6005):768-769.
908 doi:10.1126/science.1199139
- 909 10. Sharma J, Angelucci A, Sur M. Induction of visual orientation modules in auditory
910 cortex. *Nature*. 2000;404(6780):841-847. doi:10.1038/35009043
- 911 11. Lebel C, Deoni S. The development of brain white matter microstructure.
912 *NeuroImage*. 2018;182:207-218. doi:10.1016/j.neuroimage.2017.12.097
- 913 12. Kaiser M. Mechanisms of Connectome Development. *Trends in Cognitive Sciences*.
914 2017;21(9):703-717. doi:10.1016/j.tics.2017.05.010
- 915 13. The emergent properties of the connected brain | Science. Accessed November 7,
916 2023. <https://www.science.org/doi/full/10.1126/science.abq2591>

- 917 14. Forkel SJ, Friedrich P, Thiebaut de Schotten M, Howells H. White matter variability,
918 cognition, and disorders: a systematic review. *Brain Struct Funct.* 2022;227(2):529-
919 544. doi:10.1007/s00429-021-02382-w
- 920 15. Thiebaut de Schotten M, Foulon C, Nachev P. Brain disconnections link structural
921 connectivity with function and behaviour. *Nat Commun.* 2020;11(1):5094.
922 doi:10.1038/s41467-020-18920-9
- 923 16. Huber E, Donnelly PM, Rokem A, Yeatman JD. Rapid and widespread white matter
924 plasticity during an intensive reading intervention. *Nat Commun.* 2018;9(1):2260.
925 doi:10.1038/s41467-018-04627-5
- 926 17. Hutchinson EB, Schwerin SC, Avram AV, Juliano SL, Pierpaoli C. Diffusion MRI
927 and the detection of alterations following traumatic brain injury. *J Neurosci Res.*
928 2018;96(4):612-625. doi:10.1002/jnr.24065
- 929 18. Andica C, Kamagata K, Hatano T, et al. MR Biomarkers of Degenerative Brain
930 Disorders Derived From Diffusion Imaging. *J Magn Reson Imaging.*
931 2020;52(6):1620-1636. doi:10.1002/jmri.27019
- 932 19. Meijer FJA, Bloem BR, Mahlknecht P, Seppi K, Goraj B. Update on diffusion MRI
933 in Parkinson's disease and atypical parkinsonism. *J Neurol Sci.* 2013;332(1-2):21-29.
934 doi:10.1016/j.jns.2013.06.032
- 935 20. Lakhani DA, Schilling KG, Xu J, Bagnato F. Advanced Multicompartment Diffusion
936 MRI Models and Their Application in Multiple Sclerosis. *AJNR Am J Neuroradiol.*
937 2020;41(5):751-757. doi:10.3174/ajnr.A6484
- 938 21. Valdés Cabrera D, Stobbe R, Smyth P, Giuliani F, Emery D, Beaulieu C. Diffusion
939 tensor imaging tractography reveals altered fornix in all diagnostic subtypes of
940 multiple sclerosis. *Brain Behav.* 2019;10(1):e01514. doi:10.1002/brb3.1514
- 941 22. Wang L, Leonards CO, Sterzer P, Ebinger M. White matter lesions and depression: a
942 systematic review and meta-analysis. *J Psychiatr Res.* 2014;56:56-64.
943 doi:10.1016/j.jpsychires.2014.05.005
- 944 23. Tracey I, Woolf CJ, Andrews N. Composite pain biomarker signatures for objective
945 assessment and effective treatment. *Neuron.* 2019;101(5):783-800.
946 doi:10.1016/j.neuron.2019.02.019
- 947 24. Reckziegel D, Vachon-Preseau E, Petre B, Schnitzer TJ, Baliki MN, Apkarian AV.
948 Deconstructing biomarkers for chronic pain: context- and hypothesis-dependent
949 biomarker types in relation to chronic pain. *Pain.* 2019;160 Suppl 1(Suppl 1):S37-
950 S48. doi:10.1097/j.pain.0000000000001529
- 951 25. Mackey S, Greely HT, Martucci KT. Neuroimaging-based pain biomarkers:
952 definitions, clinical and research applications, and evaluation frameworks to achieve
953 personalized pain medicine. *Pain Rep.* 2019;4(4):e762.
954 doi:10.1097/PR9.0000000000000762

- 955 26. Woo CW, Chang LJ, Lindquist MA, Wager TD. Building better biomarkers: brain
956 models in translational neuroimaging. *Nat Neurosci.* 2017;20(3):365-377.
957 doi:10.1038/nn.4478
- 958 27. Mouraux A, Iannetti GD. The search for pain biomarkers in the human brain. *Brain.*
959 2018;141(12):3290-3307. doi:10.1093/brain/awy281
- 960 28. Tétreault P, Mansour A, Vachon-Presseau E, Schnitzer TJ, Apkarian AV, Baliki MN.
961 Brain Connectivity Predicts Placebo Response across Chronic Pain Clinical Trials.
962 *PLOS Biology.* 2016;14(10):e1002570. doi:10.1371/journal.pbio.1002570
- 963 29. Kutch JJ, Labus JS, Harris RE, et al. Resting-state functional connectivity predicts
964 longitudinal pain symptom change in urologic chronic pelvic pain syndrome: a
965 MAPP network study. *PAIN.* 2017;158(6):1069.
966 doi:10.1097/j.pain.0000000000000886
- 967 30. Baliki MN, Petre B, Torbey S, et al. Corticostriatal functional connectivity predicts
968 transition to chronic back pain. *Nat Neurosci.* 2012;15(8):1117-1119.
969 doi:10.1038/nn.3153
- 970 31. Kutch JJ, Ichescio E, Hampson JP, et al. Brain signature and functional impact of
971 centralized pain: a Multidisciplinary Approach to the Study of Chronic Pelvic Pain
972 (MAPP) Network Study. *Pain.* 2017;158(10):1979-1991.
973 doi:10.1097/j.pain.0000000000001001
- 974 32. Baliki MN, Schnitzer TJ, Bauer WR, Apkarian AV. Brain morphological signatures
975 for chronic pain. *PLoS One.* 2011;6(10):e26010. doi:10.1371/journal.pone.0026010
- 976 33. Henn AT, Larsen B, Frahm L, et al. Structural imaging studies of patients with
977 chronic pain: an anatomical likelihood estimate meta-analysis. *Pain.*
978 2023;164(1):e10-e24. doi:10.1097/j.pain.0000000000002681
- 979 34. Vachon-Presseau E, Tétreault P, Petre B, et al. Corticolimbic anatomical
980 characteristics predetermine risk for chronic pain. *Brain.* 2016;139(7):1958-1970.
981 doi:10.1093/brain/aww100
- 982 35. López-Solà M, Pujol J, Wager TD, et al. Altered Functional Magnetic Resonance
983 Imaging Responses to Nonpainful Sensory Stimulation in Fibromyalgia Patients.
984 *Arthritis & Rheumatology.* 2014;66(11):3200-3209. doi:10.1002/art.38781
- 985 36. Harte SE, Ichescio E, Hampson JP, et al. Pharmacologic attenuation of cross-modal
986 sensory augmentation within the chronic pain insula. *Pain.* 2016;157(9):1933-1945.
987 doi:10.1097/j.pain.0000000000000593
- 988 37. López-Solà M, Woo CW, Pujol J, et al. Towards a neurophysiological signature for
989 fibromyalgia. *Pain.* 2017;158(1):34-47. doi:10.1097/j.pain.0000000000000707

- 990 38. Baliki MN, Geha PY, Fields HL, Apkarian AV. Predicting Value of Pain and
991 Analgesia: Nucleus Accumbens Response to Noxious Stimuli Changes in the
992 Presence of Chronic Pain.
- 993 39. Baliki MN, Mansour AR, Baria AT, Apkarian AV. Functional Reorganization of the
994 Default Mode Network across Chronic Pain Conditions. *PLoS One*.
995 2014;9(9):e106133. doi:10.1371/journal.pone.0106133
- 996 40. Cheng JC, Rogachov A, Hemington KS, et al. Multivariate machine learning
997 distinguishes cross-network dynamic functional connectivity patterns in state and
998 trait neuropathic pain. *PAIN*. 2018;159(9):1764.
999 doi:10.1097/j.pain.0000000000001264
- 1000 41. Seminowicz DA, Wideman TH, Naso L, et al. Effective Treatment of Chronic Low
1001 Back Pain in Humans Reverses Abnormal Brain Anatomy and Function. *J Neurosci*.
1002 2011;31(20):7540-7550. doi:10.1523/JNEUROSCI.5280-10.2011
- 1003 42. Tétreault P, Baliki MN, Baria AT, Bauer WR, Schnitzer TJ, Apkarian AV. Inferring
1004 distinct mechanisms in the absence of subjective differences: Placebo and centrally
1005 acting analgesic underlie unique brain adaptations. *Hum Brain Mapp*.
1006 2018;39(5):2210-2223. doi:10.1002/hbm.23999
- 1007 43. Stejskal EO, Tanner JE. Spin Diffusion Measurements: Spin Echoes in the Presence
1008 of a Time-Dependent Field Gradient. *The Journal of Chemical Physics*.
1009 2004;42(1):288-292. doi:10.1063/1.1695690
- 1010 44. Tournier JD. Diffusion MRI in the brain – Theory and concepts. *Progress in Nuclear*
1011 *Magnetic Resonance Spectroscopy*. 2019;112-113:1-16.
1012 doi:10.1016/j.pnmrs.2019.03.001
- 1013 45. Moseley ME, Cohen Y, Mintorovitch J, et al. Early detection of regional cerebral
1014 ischemia in cats: Comparison of diffusion- and T2-weighted MRI and spectroscopy.
1015 *Magnetic Resonance in Medicine*. 1990;14(2):330-346.
1016 doi:10.1002/mrm.1910140218
- 1017 46. Basser PJ, Mattiello J, LeBihan D. MR diffusion tensor spectroscopy and imaging.
1018 *Biophysical Journal*. 1994;66(1):259-267. doi:10.1016/S0006-3495(94)80775-1
- 1019 47. Tournier JD, Mori S, Leemans A. Diffusion tensor imaging and beyond. *Magn Reson*
1020 *Med*. 2011;65(6):1532-1556. doi:10.1002/mrm.22924
- 1021 48. Nicholas M, Vlaeyen JWS, Rief W, et al. The IASP classification of chronic pain for
1022 ICD-11. *Pain*. 2019;160(1):28-37. doi:10.1097/j.pain.0000000000001390
- 1023 49. Treede RD, Rief W, Barke A, et al. Chronic pain as a symptom or a disease: the
1024 IASP Classification of Chronic Pain for the International Classification of Diseases
1025 (ICD-11). *Pain*. 2019;160(1):19-27. doi:10.1097/j.pain.0000000000001384

- 1026 50. Tournier JD, Yeh CH, Calamante F, Cho KH, Connelly A, Lin CP. Resolving
1027 crossing fibres using constrained spherical deconvolution: Validation using diffusion-
1028 weighted imaging phantom data. *NeuroImage*. 2008;42(2):617-625.
1029 doi:10.1016/j.neuroimage.2008.05.002
- 1030 51. Zhang H, Schneider T, Wheeler-Kingshott CA, Alexander DC. NODDI: Practical in
1031 vivo neurite orientation dispersion and density imaging of the human brain.
1032 *NeuroImage*. 2012;61(4):1000-1016. doi:10.1016/j.neuroimage.2012.03.072
- 1033 52. Smith SM, Jenkinson M, Woolrich MW, et al. Advances in functional and structural
1034 MR image analysis and implementation as FSL. *NeuroImage*. 2004;23:S208-S219.
1035 doi:10.1016/j.neuroimage.2004.07.051
- 1036 53. Smith SM, Jenkinson M, Johansen-Berg H, et al. Tract-based spatial statistics:
1037 Voxelwise analysis of multi-subject diffusion data. *NeuroImage*. 2006;31(4):1487-
1038 1505. doi:10.1016/j.neuroimage.2006.02.024
- 1039 54. O'Donnell LJ, Westin CF, Golby AJ. Tract-based morphometry for white matter
1040 group analysis. *NeuroImage*. 2009;45(3):832-844.
1041 doi:10.1016/j.neuroimage.2008.12.023
- 1042 55. Yeatman JD, Dougherty RF, Myall NJ, Wandell BA, Feldman HM. Tract Profiles of
1043 White Matter Properties: Automating Fiber-Tract Quantification. *PLOS ONE*.
1044 2012;7(11):e49790. doi:10.1371/journal.pone.0049790
- 1045 56. Zalesky A, Fornito A, Bullmore ET. Network-based statistic: Identifying differences
1046 in brain networks. *NeuroImage*. 2010;53(4):1197-1207.
1047 doi:10.1016/j.neuroimage.2010.06.041
- 1048 57. Serin E, Zalesky A, Matory A, Walter H, Kruschwitz JD. NBS-Predict: A prediction-
1049 based extension of the network-based statistic. *Neuroimage*. 2021;244:118625.
1050 doi:10.1016/j.neuroimage.2021.118625
- 1051 58. Kattem Husøy A, Eikenes L, Håberg AK, Hagen K, Stovner LJ. Diffusion tensor
1052 imaging in middle-aged headache sufferers in the general population: a cross-
1053 sectional population-based imaging study in the Nord-Trøndelag health study
1054 (HUNT-MRI). *J Headache Pain*. 2019;20(1):78. doi:10.1186/s10194-019-1028-6
- 1055 59. Zhang J, Wu YL, Su J, et al. Assessment of gray and white matter structural
1056 alterations in migraineurs without aura. *J Headache Pain*. 2017;18(1):74.
1057 doi:10.1186/s10194-017-0783-5
- 1058 60. Chong CD, Berisha V, Ross K, Kahn M, Dumkrieger G, Schwedt TJ. Distinguishing
1059 persistent post-traumatic headache from migraine: Classification based on clinical
1060 symptoms and brain structural MRI data. *Cephalalgia*. Published online April 29,
1061 2021:333102421991819. doi:10.1177/0333102421991819

- 1062 61. Marciszewski KK, Meylakh N, Di Pietro F, Macefield VG, Macey PM, Henderson
1063 LA. Fluctuating Regional Brainstem Diffusion Imaging Measures of Microstructure
1064 across the Migraine Cycle. *eNeuro*. 2019;6(4). doi:10.1523/ENEURO.0005-19.2019
- 1065 62. DaSilva AFM, Granziera C, Tuch DS, Snyder J, Vincent M, Hadjikhani N. Interictal
1066 alterations of the trigeminal somatosensory pathway and periaqueductal gray matter
1067 in migraine. *Neuroreport*. 2007;18(4):301-305.
1068 doi:10.1097/WNR.0b013e32801776bb
- 1069 63. Planchuelo-Gómez Á, García-Azorín D, Guerrero ÁL, Aja-Fernández S, Rodríguez
1070 M, de Luis-García R. Multimodal fusion analysis of structural connectivity and gray
1071 matter morphology in migraine. *Human Brain Mapping*. 2021;42(4):908-921.
1072 doi:10.1002/hbm.25267
- 1073 64. Neeb L, Bastian K, Villringer K, et al. No microstructural white matter alterations in
1074 chronic and episodic migraineurs: a case-control diffusion tensor magnetic resonance
1075 imaging study. *Headache*. 2015;55(2):241-251. doi:10.1111/head.12496
- 1076 65. Coppola G, Di Renzo A, Tinelli E, et al. Patients with chronic migraine without
1077 history of medication overuse are characterized by a peculiar white matter fiber
1078 bundle profile. *J Headache Pain*. 2020;21(1):92. doi:10.1186/s10194-020-01159-6
- 1079 66. Gomez-Beldarrain M, Oroz I, Zapirain BG, et al. Right fronto-insular white matter
1080 tracts link cognitive reserve and pain in migraine patients. *J Headache Pain*.
1081 2015;17:4. doi:10.1186/s10194-016-0593-1
- 1082 67. Szabó N, Kincses ZT, Párdutz Á, et al. White matter microstructural alterations in
1083 migraine: a diffusion-weighted MRI study. *Pain*. 2012;153(3):651-656.
1084 doi:10.1016/j.pain.2011.11.029
- 1085 68. Silvestro M, Tessitore A, Caiazzo G, et al. Disconnectome of the migraine brain: a
1086 “connectopathy” model. *J Headache Pain*. 2021;22(1):102. doi:10.1186/s10194-021-
1087 01315-6
- 1088 69. Szabó N, Kincses ZT, Párdutz A, et al. White matter disintegration in cluster
1089 headache. *The journal of headache and pain*. 2013;14:64. doi:10.1186/1129-2377-
1090 14-64
- 1091 70. Teepker M, Menzler K, Belke M, et al. Diffusion tensor imaging in episodic cluster
1092 headache. *Headache*. 2012;52(2):274-282. doi:10.1111/j.1526-4610.2011.02000.x
- 1093 71. Miller JV, Andre Q, Timmers I, et al. Subclinical post-traumatic stress
1094 symptomology and brain structure in youth with chronic headaches. *Neuroimage*
1095 *Clin*. 2021;30:102627. doi:10.1016/j.nicl.2021.102627
- 1096 72. Salomons TV, Moayed M, Weissman-Fogel I, et al. Perceived helplessness is
1097 associated with individual differences in the central motor output system. *Eur J*
1098 *Neurosci*. 2012;35(9):1481-1487. doi:10.1111/j.1460-9568.2012.08048.x

- 1099 73. Moayed M, Weissman-Fogel I, Salomons TV, et al. White matter brain and
1100 trigeminal nerve abnormalities in temporomandibular disorder. *Pain*.
1101 2012;153(7):1467-1477. doi:10.1016/j.pain.2012.04.003
- 1102 74. Gustin SM, Peck CC, Cheney LB, Macey PM, Murray GM, Henderson LA. Pain and
1103 plasticity: is chronic pain always associated with somatosensory cortex activity and
1104 reorganization? *J Neurosci*. 2012;32(43):14874-14884.
1105 doi:10.1523/JNEUROSCI.1733-12.2012
- 1106 75. Wada A, Shizukuishi T, Kikuta J, et al. Altered structural connectivity of pain-related
1107 brain network in burning mouth syndrome-investigation by graph analysis of
1108 probabilistic tractography. *Neuroradiology*. 2017;59(5):525-532.
1109 doi:10.1007/s00234-017-1830-2
- 1110 76. Khan SA, Keaser ML, Meiller TF, Seminowicz DA. Altered structure and function in
1111 the hippocampus and medial prefrontal cortex in patients with burning mouth
1112 syndrome. *Pain*. 2014;155(8):1472-1480. doi:10.1016/j.pain.2014.04.022
- 1113 77. Tan Y, Wu X, Chen J, Kong L, Qian Z. Structural and Functional Connectivity
1114 Between the Amygdala and Orbital Frontal Cortex in Burning Mouth Syndrome: An
1115 fMRI Study. *Front Psychol*. 2019;10:1700. doi:10.3389/fpsyg.2019.01700
- 1116 78. Kurokawa R, Kamiya K, Inui S, et al. Structural connectivity changes in the cerebral
1117 pain matrix in burning mouth syndrome: a multi-shell, multi-tissue-constrained
1118 spherical deconvolution model analysis. *Neuroradiology*. 2021;63(12):2005-2012.
1119 doi:10.1007/s00234-021-02732-9
- 1120 79. Dun W, Yang J, Yang L, et al. Abnormal white matter integrity during pain-free
1121 periovulation is associated with pain intensity in primary dysmenorrhea. *Brain*
1122 *Imaging Behav*. 2017;11(4):1061-1070. doi:10.1007/s11682-016-9582-x
- 1123 80. He J, Dun W, Han F, et al. Abnormal white matter microstructure along the thalamus
1124 fiber pathways in women with primary dysmenorrhea. *Brain Imaging and Behavior*.
1125 Published online 2020. doi:10.1007/s11682-020-00400-9
- 1126 81. Liu J, Liu H, Mu J, et al. Altered white matter microarchitecture in the cingulum
1127 bundle in women with primary dysmenorrhea: A tract-based analysis study. *Hum*
1128 *Brain Mapp*. 2017;38(9):4430-4443. doi:10.1002/hbm.23670
- 1129 82. Liu P, Wang G, Liu Y, et al. White matter microstructure alterations in primary
1130 dysmenorrhea assessed by diffusion tensor imaging. *Sci Rep*. 2016;6:25836.
1131 doi:10.1038/srep25836
- 1132 83. Irimia A, Labus JS, Torgerson CM, Van Horn JD, Mayer EA. Altered viscerotopic
1133 cortical innervation in patients with irritable bowel syndrome. *Neurogastroenterol*
1134 *Motil*. 2015;27(8):1075-1081. doi:10.1111/nmo.12586

- 1135 84. Ellingson BM, Mayer E, Harris RJ, et al. Diffusion tensor imaging detects
1136 microstructural reorganization in the brain associated with chronic irritable bowel
1137 syndrome. *Pain*. 2013;154(9):1528-1541. doi:10.1016/j.pain.2013.04.010
- 1138 85. Qi R, Liu C, Weng Y, et al. Disturbed Interhemispheric Functional Connectivity
1139 Rather than Structural Connectivity in Irritable Bowel Syndrome. *Front Mol*
1140 *Neurosci*. 2016;9:141. doi:10.3389/fnmol.2016.00141
- 1141 86. Hubbard CS, Becerra L, Heinz N, et al. Microstructural White Matter Abnormalities
1142 in the Dorsal Cingulum of Adolescents with IBS. *eNeuro*. 2018;5(4).
1143 doi:10.1523/ENEURO.0354-17.2018
- 1144 87. Chen JYW, Blankstein U, Diamant NE, Davis KD. White matter abnormalities in
1145 irritable bowel syndrome and relation to individual factors. *Brain Res*.
1146 2011;1392:121-131. doi:10.1016/j.brainres.2011.03.069
- 1147 88. Nan J, Zhang L, Chen Q, et al. White Matter Microstructural Similarity and Diversity
1148 of Functional Constipation and Constipation-predominant Irritable Bowel Syndrome.
1149 *J Neurogastroenterol Motil*. 2018;24(1):107-118. doi:10.5056/jnm17038
- 1150 89. Liu G, Li S, Chen N, et al. Inter-hemispheric Functional Connections Are More
1151 Vulnerable to Attack Than Structural Connection in Patients With Irritable Bowel
1152 Syndrome. *J Neurogastroenterol Motil*. 2021;27(3):426-435. doi:10.5056/jnm20134
- 1153 90. Woodworth D, Mayer E, Leu K, et al. Unique Microstructural Changes in the Brain
1154 Associated with Urological Chronic Pelvic Pain Syndrome (UCPPS) Revealed by
1155 Diffusion Tensor MRI, Super-Resolution Track Density Imaging, and Statistical
1156 Parameter Mapping: A MAPP Network Neuroimaging Study. *PLoS One*.
1157 2015;10(10):e0140250. doi:10.1371/journal.pone.0140250
- 1158 91. Huang L, Kutch JJ, Ellingson BM, et al. Brain white matter changes associated with
1159 urological chronic pelvic pain syndrome: multisite neuroimaging from a MAPP case-
1160 control study. *Pain*. 2016;157(12):2782-2791. doi:10.1097/j.pain.0000000000000703
- 1161 92. Woodworth DC, Dagher A, Curatolo A, et al. Changes in brain white matter structure
1162 are associated with urine proteins in urologic chronic pelvic pain syndrome (UCPPS):
1163 A MAPP Network study. *PLoS One*. 2018;13(12):e0206807.
1164 doi:10.1371/journal.pone.0206807
- 1165 93. Alger JR, Ellingson BM, Ashe-McNalley C, et al. Multisite, multimodal
1166 neuroimaging of chronic urological pelvic pain: Methodology of the MAPP Research
1167 Network. *Neuroimage Clin*. 2016;12:65-77. doi:10.1016/j.nicl.2015.12.009
- 1168 94. Farmer MA, Chanda ML, Parks EL, Baliki MN, Apkarian AV, Schaeffer AJ. Brain
1169 functional and anatomical changes in chronic prostatitis/chronic pelvic pain
1170 syndrome. *J Urol*. 2011;186(1):117-124. doi:10.1016/j.juro.2011.03.027

- 1171 95. Huang X, Chen J, Liu S, et al. Impaired frontal-parietal control network in chronic
1172 prostatitis/chronic pelvic pain syndrome revealed by graph theoretical analysis: A
1173 DTI study. *Eur J Neurosci.* 2021;53(4):1060-1071. doi:10.1111/ejn.14962
- 1174 96. Farmer MA, Huang L, Martucci K, et al. Brain White Matter Abnormalities in
1175 Female Interstitial Cystitis/Bladder Pain Syndrome: A MAPP Network
1176 Neuroimaging Study. *J Urol.* 2015;194(1):118-126. doi:10.1016/j.juro.2015.02.082
- 1177 97. Gupta A, Woodworth DC, Ellingson BM, et al. Disease-Related Microstructural
1178 Differences in the Brain in Women With Provoked Vestibulodynia. *J Pain.*
1179 2018;19(5):528.e1-528.e15. doi:10.1016/j.jpain.2017.12.269
- 1180 98. Mansour AR, Baliki MN, Huang L, et al. Brain white matter structural properties
1181 predict transition to chronic pain. *Pain.* 2013;154(10):2160-2168.
1182 doi:10.1016/j.pain.2013.06.044
- 1183 99. Ma J, Wang X, Qiu Q, Zhan H, Wu W. Changes in Empathy in Patients With
1184 Chronic Low Back Pain: A Structural-Functional Magnetic Resonance Imaging
1185 Study. *Front Hum Neurosci.* 2020;14:326. doi:10.3389/fnhum.2020.00326
- 1186 100. Čeko M, Shir Y, Ouellet JA, Ware MA, Stone LS, Seminowicz DA. Partial
1187 recovery of abnormal insula and dorsolateral prefrontal connectivity to cognitive
1188 networks in chronic low back pain after treatment. *Hum Brain Mapp.*
1189 2015;36(6):2075-2092. doi:10.1002/hbm.22757
- 1190 101. Kim H, Mawla I, Lee J, et al. Reduced tactile acuity in chronic low back pain is
1191 linked with structural neuroplasticity in primary somatosensory cortex and is
1192 modulated by acupuncture therapy. *Neuroimage.* 2020;217:116899.
1193 doi:10.1016/j.neuroimage.2020.116899
- 1194 102. Bishop JH, Shpaner M, Kubicki A, Clements S, Watts R, Naylor MR. Structural
1195 network differences in chronic musculoskeletal pain: Beyond fractional anisotropy.
1196 *Neuroimage.* 2018;182:441-455. doi:10.1016/j.neuroimage.2017.12.021
- 1197 103. Lieberman G, Shpaner M, Watts R, et al. White matter involvement in chronic
1198 musculoskeletal pain. *J Pain.* 2014;15(11):1110-1119.
1199 doi:10.1016/j.jpain.2014.08.002
- 1200 104. Cruz-Almeida Y, Coombes S, Febo M. Pain Differences in Neurite Orientation
1201 and Dispersion Density Imaging Measures Among Community-Dwelling Older
1202 Adults. *Exp Gerontol.* 2021;154:111520. doi:10.1016/j.exger.2021.111520
- 1203 105. Pijnenburg M, Hosseini SMH, Brumagne S, Janssens L, Goossens N,
1204 Caeyenberghs K. Structural Brain Connectivity and the Sit-to-Stand-to-Sit
1205 Performance in Individuals with Nonspecific Low Back Pain: A Diffusion Magnetic
1206 Resonance Imaging-Based Network Analysis. *Brain Connect.* 2016;6(10):795-803.
1207 doi:10.1089/brain.2015.0401

- 1208 106. Coppieters I, De Pauw R, Caeyenberghs K, et al. Differences in white matter
1209 structure and cortical thickness between patients with traumatic and idiopathic
1210 chronic neck pain: Associations with cognition and pain modulation? *Hum Brain*
1211 *Mapp.* 2018;39(4):1721-1742. doi:10.1002/hbm.23947
- 1212 107. Butler S, Landmark T, Glette M, Borchgrevink P, Woodhouse A. Chronic
1213 widespread pain-the need for a standard definition. *Pain.* 2016;157(3):541-543.
1214 doi:10.1097/j.pain.0000000000000417
- 1215 108. Sundgren PC, Petrou M, Harris RE, et al. Diffusion-weighted and diffusion tensor
1216 imaging in fibromyalgia patients: a prospective study of whole brain diffusivity,
1217 apparent diffusion coefficient, and fraction anisotropy in different regions of the
1218 brain and correlation with symptom severity. *Acad Radiol.* 2007;14(7):839-846.
1219 doi:10.1016/j.acra.2007.03.015
- 1220 109. Ceko M, Bushnell MC, Fitzcharles MA, Schweinhardt P. Fibromyalgia interacts
1221 with age to change the brain. *Neuroimage Clin.* 2013;3:249-260.
1222 doi:10.1016/j.nicl.2013.08.015
- 1223 110. Kim H, Kim J, Loggia ML, et al. Fibromyalgia is characterized by altered frontal
1224 and cerebellar structural covariance brain networks. *Neuroimage Clin.* 2015;7:667-
1225 677. doi:10.1016/j.nicl.2015.02.022
- 1226 111. Hadanny A, Bechor Y, Catalogna M, et al. Hyperbaric Oxygen Therapy Can
1227 Induce Neuroplasticity and Significant Clinical Improvement in Patients Suffering
1228 From Fibromyalgia With a History of Childhood Sexual Abuse-Randomized
1229 Controlled Trial. *Front Psychol.* 2018;9:2495. doi:10.3389/fpsyg.2018.02495
- 1230 112. Fayed N, Garcia-Campayo J, Magallón R, et al. Localized 1H-NMR spectroscopy
1231 in patients with fibromyalgia: a controlled study of changes in cerebral
1232 glutamate/glutamine, inositol, choline, and N-acetylaspartate. *Arthritis Res Ther.*
1233 2010;12(4):R134. doi:10.1186/ar3072
- 1234 113. Lutz J, Jäger L, de Quervain D, et al. White and gray matter abnormalities in the
1235 brain of patients with fibromyalgia: a diffusion-tensor and volumetric imaging study.
1236 *Arthritis Rheum.* 2008;58(12):3960-3969. doi:10.1002/art.24070
- 1237 114. Birklein F, Schlereth T. Complex regional pain syndrome-significant progress in
1238 understanding. *Pain.* 2015;156 Suppl 1:S94-S103.
1239 doi:10.1097/01.j.pain.0000460344.54470.20
- 1240 115. Bruehl S. Complex regional pain syndrome. *BMJ.* 2015;351:h2730.
1241 doi:10.1136/bmj.h2730
- 1242 116. Hotta J, Zhou G, Harno H, Forss N, Hari R. Complex regional pain syndrome:
1243 The matter of white matter? *Brain Behav.* 2017;7(5):e00647. doi:10.1002/brb3.647
- 1244 117. Geha PY, Baliki MN, Harden RN, Bauer WR, Parrish TB, Apkarian AV. The
1245 brain in chronic CRPS pain: Abnormal gray-white matter interactions in emotional

- 1246 and autonomic regions. *Neuron*. 2008;60(4):570-581.
1247 doi:10.1016/j.neuron.2008.08.022
- 1248 118. Jennings RG, Van Horn JD. Publication bias in neuroimaging research:
1249 Implications for meta-analyses. *Neuroinformatics*. 2012;10(1):67-80.
1250 doi:10.1007/s12021-011-9125-y
- 1251 119. Cahn AJ, Little G, Beaulieu C, Tétreault P. Diffusion properties of the fornix
1252 assessed by deterministic tractography shows age, sex, volume, cognitive,
1253 hemispheric, and twin relationships in young adults from the Human Connectome
1254 Project. *Brain Struct Funct*. 2021;226(2):381-395. doi:10.1007/s00429-020-02181-9
- 1255 120. Cai LY, Yang Q, Kanakaraj P, et al. MASiVar: Multisite, multiscanner, and
1256 multisubject acquisitions for studying variability in diffusion weighted MRI. *Magn
1257 Reson Med*. 2021;86(6):3304-3320. doi:10.1002/mrm.28926
- 1258 121. Burdette JH, Durden DD, Elster AD, Yen YF. High b-value diffusion-weighted
1259 MRI of normal brain. *J Comput Assist Tomogr*. 2001;25(4):515-519.
1260 doi:10.1097/00004728-200107000-00002
- 1261 122. Lebel C, Gee M, Camicioli R, Wieler M, Martin W, Beaulieu C. Diffusion tensor
1262 imaging of white matter tract evolution over the lifespan. *Neuroimage*.
1263 2012;60(1):340-352. doi:10.1016/j.neuroimage.2011.11.094
- 1264 123. Ni H, Kavcic V, Zhu T, Ekholm S, Zhong J. Effects of Number of Diffusion
1265 Gradient Directions on Derived Diffusion Tensor Imaging Indices in Human Brain.
1266 *AJNR Am J Neuroradiol*. 2006;27(8):1776-1781.
- 1267 124. Oouchi H, Yamada K, Sakai K, et al. Diffusion Anisotropy Measurement of Brain
1268 White Matter Is Affected by Voxel Size: Underestimation Occurs in Areas with
1269 Crossing Fibers. *AJNR Am J Neuroradiol*. 2007;28(6):1102-1106.
1270 doi:10.3174/ajnr.A0488
- 1271 125. Wu YC, Alexander AL. Hybrid diffusion imaging. *Neuroimage*. 2007;36(3):617-
1272 629. doi:10.1016/j.neuroimage.2007.02.050
- 1273 126. Basser PJ, Mattiello J, LeBihan D. Estimation of the effective self-diffusion
1274 tensor from the NMR spin echo. *J Magn Reson B*. 1994;103(3):247-254.
1275 doi:10.1006/jmrb.1994.1037
- 1276 127. Shragar RI, Basser PJ. Anisotropically weighted MRI. *Magn Reson Med*.
1277 1998;40(1):160-165. doi:10.1002/mrm.1910400121
- 1278 128. Jeurissen B, Descoteaux M, Mori S, Leemans A. Diffusion MRI fiber
1279 tractography of the brain. *NMR in Biomedicine*. 2019;32(4):e3785.
1280 doi:10.1002/nbm.3785
- 1281 129. Dell'Acqua F, Tournier JD. Modelling white matter with spherical deconvolution:
1282 How and why? *NMR in Biomedicine*. 2019;32(4):e3945. doi:10.1002/nbm.3945

- 1283 130. Neher P, Stieltjes B, Wolf I, Meinzer HP, Maier-Hein K. Analysis of tractography
1284 biases introduced by anisotropic voxels. In: ; 2013.
- 1285 131. Tax CMW, Bastiani M, Veraart J, Garyfallidis E, Okan Irfanoglu M. What's new
1286 and what's next in diffusion MRI preprocessing. *Neuroimage*. 2022;249:118830.
1287 doi:10.1016/j.neuroimage.2021.118830
- 1288 132. De Luca A, Ianus A, Leemans A, et al. On the generalizability of diffusion MRI
1289 signal representations across acquisition parameters, sequences and tissue types:
1290 Chronicles of the MEMENTO challenge. *NeuroImage*. 2021;240:118367.
1291 doi:10.1016/j.neuroimage.2021.118367
- 1292 133. Diffusion MRI microstructure models with in vivo human brain Connectome
1293 data: results from a multi-group comparison - Ferizi - 2017 - NMR in Biomedicine -
1294 Wiley Online Library. Accessed December 14, 2023.
1295 <https://analyticalsciencejournals.onlinelibrary.wiley.com/doi/10.1002/nbm.3734>
- 1296 134. Pizzolato M, Palombo M, Bonet-Carne E, et al. Acquiring and Predicting
1297 Multidimensional Diffusion (MUDI) Data: An Open Challenge. In: Bonet-Carne E,
1298 Hutter J, Palombo M, Pizzolato M, Seppehrband F, Zhang F, eds. *Computational*
1299 *Diffusion MRI*. Mathematics and Visualization. Springer International Publishing;
1300 2020:195-208. doi:10.1007/978-3-030-52893-5_17
- 1301 135. Smith SM, Jenkinson M, Johansen-Berg H, et al. Tract-based spatial statistics:
1302 voxelwise analysis of multi-subject diffusion data. *Neuroimage*. 2006;31(4):1487-
1303 1505. doi:10.1016/j.neuroimage.2006.02.024
- 1304 136. Bach M, Laun FB, Leemans A, et al. Methodological considerations on tract-
1305 based spatial statistics (TBSS). *NeuroImage*. 2014;100:358-369.
1306 doi:10.1016/j.neuroimage.2014.06.021
- 1307 137. Leemans A, Jeurissen B, Sijbers J, Jones DK. ExploreDTI: A graphical toolbox
1308 for processing, analyzing, and visualizing diffusion MR data. *17th Annual Meeting of*
1309 *Intl Soc Mag Reson Med*. 2009;17.
- 1310 138. Tournier JD, Smith R, Raffelt D, et al. MRtrix3: A fast, flexible and open
1311 software framework for medical image processing and visualisation. *Neuroimage*.
1312 2019;202:116137. doi:10.1016/j.neuroimage.2019.116137
- 1313 139. Karlsgodt KH, John M, Ikuta T, et al. The accumbens tract: Diffusion tensor
1314 imaging characterization and developmental change from childhood to adulthood.
1315 *Human Brain Mapping*. 2015;36(12):4954. doi:10.1002/hbm.22989
- 1316 140. Davis KD, Aghaeepour N, Ahn AH, et al. Discovery and validation of biomarkers
1317 to aid the development of safe and effective pain therapeutics: challenges and
1318 opportunities. *Nat Rev Neurol*. 2020;16(7):381-400. doi:10.1038/s41582-020-0362-2

- 1319 141. Sluka KA, Wager TD, Sutherland SP, et al. Predicting chronic postsurgical pain:
1320 current evidence and a novel program to develop predictive biomarker signatures.
1321 *PAIN*. 2023;164(9):1912. doi:10.1097/j.pain.0000000000002938
- 1322 142. Assaf Y, Johansen-Berg H, Thiebaut de Schotten M. The role of diffusion MRI in
1323 neuroscience. *NMR Biomed*. 2019;32(4):e3762. doi:10.1002/nbm.3762
- 1324 143. Jeurissen B, Leemans A, Tournier J, Jones DK, Sijbers J. Investigating the
1325 prevalence of complex fiber configurations in white matter tissue with diffusion
1326 magnetic resonance imaging. *Hum Brain Mapp*. 2013;34(11):2747-2766.
1327 doi:10.1002/hbm.22099
- 1328 144. Gorgolewski KJ, Auer T, Calhoun VD, et al. The brain imaging data structure, a
1329 format for organizing and describing outputs of neuroimaging experiments. *Sci Data*.
1330 2016;3(1):160044. doi:10.1038/sdata.2016.44
- 1331 145. Gorgolewski KJ, Varoquaux G, Rivera G, et al. NeuroVault.org: A repository for
1332 sharing unthresholded statistical maps, parcellations, and atlases of the human brain.
1333 *NeuroImage*. 2016;124:1242-1244. doi:10.1016/j.neuroimage.2015.04.016
- 1334 146. Orhac F, Eertink JJ, Cottureau AS, et al. A Guide to ComBat Harmonization of
1335 Imaging Biomarkers in Multicenter Studies. *J Nucl Med*. 2022;63(2):172-179.
1336 doi:10.2967/jnumed.121.262464
- 1337 147. Mirzaalian H, de Pierrefeu A, Savadjiev P, et al. Harmonizing Diffusion MRI
1338 Data Across Multiple Sites and Scanners. *Med Image Comput Comput Assist Interv*.
1339 2015;9349:12-19. doi:10.1007/978-3-319-24553-9_2
- 1340 148. Jones DK, Cercignani M. Twenty-five pitfalls in the analysis of diffusion MRI
1341 data. *NMR Biomed*. 2010;23(7):803-820. doi:10.1002/nbm.1543
- 1342